quite simply. The difference arises from a change in electron-electron scattering which accompanies a change in the occupation of d states. The rigid-band model thus provides an adequate basis for explaining the difference in photoemission in Ni and Ni–Al alloys, just as it has been used successfully to explain the magnetic behavior of Ni–Al alloys.

Inelastically scattered electrons contribute about 15% to the total energy distribution and about 20% to the low-energy peak at $h\nu = 10.2$ eV for pure Ni. Values of the mean free paths for electron-electron scattering for electrons 7 eV above the Fermi energy are about 70 and 100 Å, respectively, for pure Ni and 92%-Ni alloy.

PHYSICAL REVIEW VOLUME 165, NUMBER 2 10 JANUARY 1968

Cumulant Expansion of Localized-Electron Model for Antiferromagnetic Insulators*

TADASHI ARAI
Argonne National Laboratory, Argonne, Illinois
(Received 2 June 1967)

A many-body perturbation theory is developed for the calculation of the antiferromagnetic ground state and lower excited states of one-electron atoms in the insulating state. It is assumed that the interatomic distances are moderately small and that the interactions are well described by exchange coupling, but that distortion of atoms in the lattice is still negligible. The method is essentially the Heitler-London approach: A set of Slater determinants is constructed from nonorthogonal atomic orbitals with all possible spin arrangements. The unperturbed ground state $|0\rangle$ has an alternating spin configuration, while excited states are generated one by one from $|0\rangle$ by interchanges of spins and by projecting out the lower excited states. The resulting orthonormal states introduce the concept of quasielectron (or quasihole) states and define creation and destruction operators of those quasiparticles. Although the quasiparticles are correlated with each other through the overlap integrals in the projected wave functions, the energy matrix elements can be decomposed into linked clusters of localized electrons and holes. It is found that the clusters thus generated are cumulants. The expression for the energy matrix is then transformed into the form of an effective Hamiltonian consisting of cumulants and of creation and destruction operators of quasifermions, and the concept of the exchange interaction is defined in terms of those operators. The new formulation not only facilitates the use of the familiar many-body perturbation theory, but also eliminates difficulties in handling spin variables in the Heisenberg theory of magnetism. If only the two-body Coulomb and exchange diagrams are retained and the higher-order diagrams are neglected, however, the effective Hamiltonian takes a form reminiscent of the anisotropic exchange Hamiltonian, $H_{\text{spin}} = -\sum_{k,h} J_{kh}[S_k^z S_h^z + \lambda(S_k^x S_h^x + S_k^y S_h^y)]$, which is used in the generalized Heisenberg theory and which includes the Ising model in its limit $\lambda \to 0$. Finally, it is shown that excitations accompanying electron transfers are readily included in the present method as additional diagrams by an extension of the prescriptions for the generation of excited spin states. This yields, in its first approximation, the intra-atomic interaction and the electron-transfer interaction, leading to the Hamiltonian assumed by Hubbard and Anderson.

I. INTRODUCTION

EXCHANGE coupling between atoms has been a subject of considerable discussion in the theory of magnetism, but the treatments are mostly based on unrealistic and inconsistent approximations.[1] First of all, the explicit consequences of having many atoms in a lattice have been neglected. This would not be inappropriate for a system of weakly interacting atoms in the limit of large interatomic distances, but such a situation is rarely applicable to real magnetic materials since atoms in solids interact rather strongly with each other. Furthermore, if atoms are truly well-separated, the van der Waals interaction will dominate over the short-range exchange interaction, and the Heitler-London method is not even asymptotically correct in the calculation of exchange coupling.[2,3] However, the effect of the long-range interaction has often been neglected.

The effect of distant atoms appears through the overlapping of atomic wave functions, but the nonorthogonality of the latter introduces numerous complications in the reduction of the energy expression, and only recently, has such a reduction been performed rigorously.[4–6] Use of orthogonal functions as atomic bases is, of course, undesirable because it yields the false con-

* Based on work performed under the auspices of the U.S. Atomic Energy Commission.

[1] For a complete review of this topic see C. Herring, in *Magnetism*, edited by G. T. Rado and H. Shul (Academic Press Inc., New York, 1966), Vol. IIB.

[2] C. Herring, Rev. Mod. Phys. **34**, 631 (1962).

[3] L. P. Gor'kov and L. P. Pitaevskii, Dokl. Akad. Nauk SSSR **151**, 822 (1963) [English transl.: Soviet Phys.—Doklady **8**, 788 (1964)]; C. Herring and M. Flicker, Phys. Rev. **134**, A362 (1964).

[4] T. Arai, Phys. Rev. **126**, 471 (1962); **134**, A824 (1964).

[5] W. J. Mullin, Phys. Rev. **136**, A1126 (1964).

[6] F. Yonezawa, Progr. Theoret. Phys. (Kyoto) **34**, 210 (1965). See the criticism on this paper by T. Arai, *ibid.* **36**, 473 (1966).

clusion that the ground state of one-electron atoms is always in the ferromagnetic state.

Furthermore, if we project out the motion of electrons into spin space and generate a spin Hamiltonian, only exchange interaction between atoms remains, and more dynamical interactions such as electron transfers and excitations of atoms can never be taken into consideration. All previous work[4–6] is limited in scope due to this restriction.

To circumvent those difficulties, we shall present in this paper a method of calculating the antiferromagnetic ground state and lower excited states of one-electron atoms in the insulating state. The formulation will be developed for the situation where the interatomic distances are moderately small and the interactions are well described by exchange coupling but distortions of atoms are still small. The method is, in fact, a many-body perturbation expansion based on the Heitler-London approach,[7] but handles the localized electrons explicitly without projecting out into spin space. This procedure enables us to include electron transfers and excitations of atoms. In fact, the method developed here could become a rigorous one which is comparable to the many-body perturbation treatment of the band theory.

To simplify the formulation, we shall treat, in the main part of this paper, *the simple Heitler-London case* where each atom carries a single localized electron and where no electron transfers nor excitations of atoms are included. In Sec. VII, however, we shall show that electron transfers can be taken into account easily by relaxing the restrictions imposed on the prescriptions for generation of diagrams. Excitations of atoms may also be considered in the method by adding more basic functions, but the extension is only a technical matter, and we shall not describe it any further.

As we shall discuss in Sec. VII, even the result of the simple Heitler-London case given by (7.4) will be different from and more general than the previous work,[4–6] since our result can be written in a form reminiscent of the anisotropic exchange interaction:

$$H_{\rm spin}(\lambda) = -\sum_{k,h} J_{kh}[S_k^z S_h^z + \lambda(S_k^x S_h^x + S_k^y S_h^y)], \tag{1.1}$$

while the previous work could cover only the isotropic case where $\lambda = 1$. The constants J_{kh} and λJ_{kh} may also be interpreted differently. The λJ_{kh} represents the *exchange coupling* given by a matrix element between two states which are generated by an interchange of electrons, while the first term in (1.1), $-\sum_{k,h} J_{kh} S_k^z S_h^z$, may be considered as a *static interaction* between classical spins. If the exchange diagrams are negligible as compared with the Coulomb interaction, it is entirely plausible that the parameter λ vanishes, suggesting a possibility of finding the Ising interaction in real magnetic materials.

It should be noted here that an expression like the anisotropic spin Hamiltonian (1.1) was obtained from the effective Hamiltonian (7.4) by inserting appropriate atomic spin operators in place of the creation and destruction operators of electrons. Although this was instructive for the forgoing illustration, the replacement is not rigorous because the basic functions used here are correlated wave functions of electrons and different from the spin functions assumed in the Heisenberg theory. In fact, the effective Hamiltonian generated from (7.4) and containing only the two-body Coulomb and exchange diagrams could still be spin isotropic despite the similarity in appearance to the anisotropic spin Hamiltonian.

The electron-transfer mechanism yields new types of interactions such as the intra-atomic interaction and the electron-transfer interaction. Those interactions are postulated, for instance, in Hubbard's theory[8] of narrow bands and Anderson's theory[9] of localized moments, but the present method provides an explicit prescription for the calculation of the constants. We note that those interactions are not expressible in terms of atomic spin operators and hence cannot be considered in the Heisenberg theory.

Since the formulation of the method involves complicated mathematics, we shall sketch the structure of the paper in the following. In Sec. II, we shall construct a set of Slater determinants from nonorthogonal atomic orbitals with all possible spin arrangements. The unperturbed ground-state wave function $|0\rangle$ has an alternating spin arrangement while other functions $|nmp\rangle$ are generated from $|0\rangle$ by interchanges of m pairs of α and β spins and n flips of β spins (or α spins). In Sec. IV, functions $|nmp\rangle$ with common n and m will be orthogonalized to each other after projecting out the lower components $|nm'p'\rangle$ with $m' < m$. The resulting orthonormal functions $\mathfrak{N}|nmp\rangle$ will describe the spin densities which are schematically represented by the spin functions of the original bases $|nmp\rangle$. The concept of quasielectron (or quasihole) states as well as the definition of creation and destruction operators of those quasiparticles will follow from the orthonormal functions $\mathfrak{N}|nmp\rangle$.

Although the quasiparticles are correlated with each other through the overlap integrals involved in $\mathfrak{N}|nmp\rangle$, the decomposition of the energy matrix elements into linked clusters can be performed rigorously. This will be the subject of Secs. III–VI. Finally, it will be found that the linked clusters so generated are cumulants. In Sec. VII, the expression of the energy matrix will be transformed into the form of an effective Hamiltonian consisting of cumulant integrals and creation and destruction operators of quasiparticles. This facilitates

[7] See also a perturbation expansion developed by W. J. Carr, Jr., Phys. Rev. **131**, 1947 (1963). Most of his equations, however, were specialized for the case of nondegenerate atoms.

[8] J. Hubbard, Proc. Roy. Soc. (London) **A276**, 238 (1963); **A277**, 237 (1964); **A281**, 401 (1964); **A285**, 542 (1965).

[9] P. W. Anderson, Phys. Rev. **124**, 41 (1961).

the use of the familiar many-body perturbation theory.[10–12]

II. BASIC WAVE FUNCTIONS

Let us consider a lattice of $2N$ one-electron atoms. At infinite separations, the ground state of this lattice has 2^{2N}-fold degeneracy. As the interatomic distances R are decreased, this degeneracy will split up, but if N is not too large and if the R's are not too small, there will be a set of 2^{2N} lowest levels well separated from more highly excited states. For the most part of this paper, we calculate the ground state and lower excited states among the 2^{2N} levels assuming that those lower states are still well separated from the *more highly excited states*, even though N is infinitely large and the distances R are moderately small. Spin-wave states in many antiferromagnetic insulators are considered to satisfy this situation. The system is then described by a set of Heitler-London functions

$$|\,nmp\rangle\equiv\{(2N)!c\}^{-1/2}\epsilon_{nmp}\sum_P(-1)^P \times P_r\Phi(1,2,\cdots,2N)P_\sigma\Theta_{nmp}(1,2,\cdots,2N), \quad (2.1)$$

associated with a set of 2^{2N} functions Θ_{nmp} for $2N$ spins and the product Φ of $2N$ atomic orbitals:

$$\Phi(1,2,\cdots,2N)\equiv\varphi\{r_1-R(1^A)\}\cdots\varphi\{r_N-R(N^A)\} \times\varphi\{r_{N+1}-R(1^B)\}\cdots\varphi\{r_{2N}-R(N^B)\}, \quad (2.2)$$

where

$$|\,h^A)\equiv\varphi\{r-R(h^A)\} \quad (2.3a)$$

and

$$|\,k^B)\equiv\varphi\{r-R(k^B)\} \quad (2.3b)$$

are the atomic orbitals centered at the lattice points $R(h^A)\equiv R_h$ and $R(k^B)\equiv R_k$, respectively. In (2.1), P_r and P_σ are permutation operators of the positional and spin coordinates r and σ, respectively, and the constant c and the sign $\epsilon_{nmp}=\pm1$ will be specified later.

For convenience, we introduce a two-sublattice structure such that the nearest neighbors of an atom on sublattice $[A]$ are on sublattice $[B]$ and vice versa. This distinction of lattice points has already been incorporated in the notation of atomic orbitals $|\,h^A)$ and $|\,k^B)$. For example, the h^A indicates the hth atom on $[A]$ and so on. By Θ_0, we denote the unperturbed ground-state spin function in which all atoms on sublattice $[A]$ are in spin-up states α and all on $[B]$ in spin-down states β:

$$\Theta_0=\alpha(\sigma_1,1^A)\cdots\alpha(\sigma_N,N^A)\beta(\sigma_{N+1},1^B)\cdots\beta(\sigma_{2N},N^B). \quad (2.4)$$

Other $2^{2N}-1$ states can be generated from Θ_0 by taking all possible ways of reversing spins on $[A]$ and $[B]$, that is,

$$\Theta_{nmp}\equiv S_{nmp}\Theta_0 \equiv S^-(h_1^A)\cdots S^-(h_m^A)\,S^+(k_1^B)\cdots S^+(k_{m+n}^B)\Theta_0, \quad (2.5)$$

where $S^\pm(h^A)$ is the raising or lowering operator of the spin at atom h^A on $[A]$:

$$S^\pm(h^A)=S^x(h^A)\pm iS^y(h^A), \quad (2.6)$$

and S_{nmp} represents the product of $S^-(h^A)$'s and $S^+(k^B)$'s.

Since the spin functions Θ_{nmp} are single products of α's and β's, the wave functions $|\,nmp\rangle$ generated by (2.1) are also written as single Slater determinants. To facilitate the matrix calculation, let us separate the subspace spanned by orbitals with α spins from the subspace consisting of orbitals with β spins and denote the α-spin subspace by G_α. Similarly, the subspace G_β consists of orbitals with β spins. The operation S_{nmp} introduced in (2.5) is then equivalent to the rearrangement of orbitals where orbitals $|\,h_1^A)\cdots|\,h_m^A)$ are transferred from G_α to G_β and at the same time $|\,k_1^B)\cdots|\,k_{m+n}^B)$ from G_β to G_α. When $n\geq0$, the function $|\,nmp\rangle$ is written as

$$|\,nmp\rangle=\{(2N)!c\}^{-1/2}\sum_P(-1)^PP \times\Phi_A[k_1^B\cdots k_{m+n}^B;\,h_1^A\cdots h_m^A] \times\Phi_B[h_1^A\cdots h_m^A;\,k_1^B\cdots k_{m+n}^B] \times\alpha(\sigma_1)\cdots\alpha(\sigma_{N+n})\beta(\sigma_{N+n+1})\cdots\beta(\sigma_{2N}), \quad (2.7)$$

where $\Phi_B[h_1^A\cdots h_m^A;\,k_1^B\cdots k_{m+n}^B]$ is obtained from the product of N orbitals $\Phi_B=|\,1^B)\cdots|\,N^B)$ by the replacement of $|\,k_1^B)\cdots|\,k_m^B)$ by $|\,h_1^A)\cdots|\,h_m^A)$, together with the deletion of $|\,k_{m+1}^B)\cdots|\,k_{m+n}^B)$. Similarly, $\Phi_A[k_1^B\cdots k_{m+n}^B;\,h_1^A\cdots h_m^A]$ is derived from the original product Φ_A by the replacement of m orbitals and by the addition of $|\,k_{m+1}^B)\cdots|\,k_{m+n}^B)$. When $n<0$, the expressions for G_α and G_β are reversed.

The expression for $|\,nmp\rangle$ given in (2.7) is not unique since a number of ways exists to construct pairing of k's and h's, but all functions generated from a fixed S_{nmp} are the same up to the order of permutations. A possible ambiguity in sign may be eliminated by the following counting procedure. Instead of deleting $|\,k_{m+1}^B)\cdots|\,k_{m+n}^B)$ in Φ_B immediately, let us replace them by fictitious functions $\delta(k_{m+1}^B),\cdots,\delta(k_{m+n}^B)$. The summation $\sum_P$ should be extended over $2N+n$ functions, but the new expression is now determined uniquely including the sign. For example, let us consider a function obtained from (2.7) by the replacement of $k_1^B\cdots k_{m+n}^B$ by $k_{p_1}^B\cdots k_{p_{m+n}}^B$, where the series $p_1,\cdots,p_{m+n}$ is generated from $1,\cdots,m+n$ by the permutation P. The new expression for the G_α can be transformed back to the original form by the permu-

[10] J. Goldstone, Proc. Roy. Soc. (London) **A239**, 267 (1957); J. Hubbard, *ibid.* **A240**, 539 (1957).
[11] R. Kubo, J. Phys. Soc. Japan **17**, 1100 (1962).
[12] T. Arai and B. Goodman, Phys. Rev. **155**, 514 (1967).

tation P_φ^{-1} of atomic orbitals while the G_β part returns to the expression in (2.7) by the permutation P_τ^{-1} of electron coordinates. Since the total permutation $P_\varphi^{-1}\times P_\tau^{-1}$ is always even, the functions generated should carry a fixed sign regardless of the pairing method. Since the δ functions are assumed to be orthogonal to each other as well as to all atomic orbitals $|\,h^A\rangle$ and $|\,k^B\rangle$ involved, the replacement by δ is effectively equivalent to the deletion of $|\,k_{m+1}{}^B\rangle, \cdots, |\,k_{m+n}{}^B\rangle$ in Φ_B when the matrix is integrated. In fact, the δ functions are designed to fix the sign of $|\,nmp\rangle$ uniquely and should be removed after establishing the sign.

The sign ϵ_{nmp} in (2.1) is determined in accordance with (2.7), and the constant c is fixed so that the unperturbed ground-state function $|\,0\rangle\equiv|\,001\rangle$ is normalized to 1:

$$\langle 0\,|\,0\rangle=1. \tag{2.8}$$

III. EXPANSION OF OVERLAP MATRIX ELEMENTS

The use of nonorthogonal atomic orbitals as basis necessarily introduces the nonorthogonality among wave functions $|\,nmp\rangle$ with a fixed n obtained by (2.7). As electrons involved in $|\,nmp\rangle$ are correlated among each other through the overlap integrals and electron interchanges are controlled by the value of the overlap matrix $\langle\Delta\rangle$, it is important to calculate $\langle\Delta\rangle$ correctly.

Since the wave functions are single Slater determinants, the overlap matrix $\langle\Delta\rangle$ splits into two determinants belonging to subspaces G_α and G_β, as follows.

$$\langle nm'p'\,|\,nmp\rangle=\langle nm'A_{p'}\,|\,nmA_p\rangle\langle -nm'B_{p'}\,|\,-nmB_p\rangle, \tag{3.1}$$

where

$$\langle nm'A_{p'}\,|\,nmA_p\rangle=c_A^{-1}\int\sum_P(-1)^P P_\tau\Phi_A^*[k_1{}'^B\cdots k_{m'+n}{}'^B;\,h_1{}'^A\cdots h_{m'}{}'^A]\Phi_A[k_1{}^B\cdots k_{m+n}{}^B;\,h_1{}^A\cdots h_m{}^A]d\tau, \tag{3.2a}$$

and

$$\langle -nm'B_{p'}\,|\,-nmB_p\rangle=c_B^{-1}\int\sum_P(-1)^P P_\tau\Phi_B^*[h_1{}'^A\cdots h_{m'}{}'^A;\,k_1{}'^B\cdots k_{m'+n}{}'^B]\Phi_B[h_1{}^A\cdots h_m{}^A;\,k_1{}^B\cdots k_{m+n}{}^B]d\tau. \tag{3.2b}$$

The constants c_A and c_B are chosen so that $\langle 0A\,|\,0A\rangle\equiv\langle 00A_1\,|\,00A_1\rangle=1$, $\langle 0B\,|\,0B\rangle\equiv\langle 00B_1\,|\,00B_1\rangle=1$, and $c=c_Ac_B$.

We note that $\langle 0A\,|\,0A\rangle$ and $\langle 0B\,|\,0B\rangle$ are both written in the form of determinants Δ_A and Δ_B, whose $h'h$ and $k'k$ elements are given by the overlap integrals $(h'^A\,|\,h^A)$ and $(k'^B\,|\,k^B)$, respectively; of course, the values of Δ_A and Δ_B are unity due to the normalization constants c_A and c_B. In the following, we shall show that other elements $\langle nm'A_{p'}\,|\,nmA_p\rangle$ and $\langle -nm'B_{p'}\,|\,-nmB_p\rangle$ can be expanded in terms of signed minors of the determinants Δ_A and Δ_B. To illustrate electron interchanges involved in those elements explicitly, let us denote the expressions in (3.2) as follows:

$$\langle nm'A_{p'}\,|\,nmA_p\rangle\equiv\langle k_1{}'^B\cdots k_{m'+n}{}'^B;\,h_1{}'^A\cdots h_{m'}{}'^A\,|\,k_1{}^B\cdots k_{m+n}{}^B;\,h_1{}^A\cdots h_m{}^A\rangle, \tag{3.3a}$$

and

$$\langle -nm'B_{p'}\,|\,-nmB_p\rangle\equiv\langle h_1{}'^A\cdots h_{m'}{}'^A;\,k_1{}'^B\cdots k_{m'+n}{}'^B\,|\,h_1{}^A\cdots h_m{}^A;\,k_1{}^B\cdots k_{m+n}{}^B\rangle, \tag{3.3b}$$

where the type of interchanges described in (2.7) is assumed for the first m (or m') pairs h_ik_i, $i=1, 2, \cdots, m$ (or m').

Let us demonstrate the calculation with simple examples.

(i) For instance, the element $\langle 0\,|\,k^B;h^A\rangle\equiv\langle 0A\,|\,01A\rangle$ with $S_{01}=S^-(h^A)S^+(k^B)$ is obtained from the determinant Δ_A by replacing the component $|\,h^A)$ by $|\,k^B)$. This replacement can take place conveniently in the familiar expansion of a determinant:

$$1=\Delta_A=\sum_l(h^A\,|\,\Delta^{-1}\,|\,l^A)\,(l^A\,|\,h^A) \tag{3.4}$$

in terms of *cofactors* $(h^A\,|\,\Delta^{-1}\,|\,l^A)$ of elements $(l^A\,|\,h^A)$ in Δ_A. The result is

$$\langle 0\,|\,k^B;h^A\rangle=\sum_l(h^A\,|\,\Delta^{-1}\,|\,l^A)\,(l^A\,|\,k^B). \tag{3.5}$$

(ii) The replacement of $(h^A\,|$ by $(k^B\,|$ in the expansion

$$1=\Delta_A=\sum_l(h^A\,|\,l^A)\,(l^A\,|\,\Delta^{-1}\,|\,h^A) \tag{3.6}$$

will yield the expression for $\langle k^B;h^A\,|\,0\rangle$:

$$\langle k^B;h^A\,|\,0\rangle=\sum_l(k^B\,|\,l^A)\,(l^A\,|\,\Delta^{-1}\,|\,h^A). \tag{3.7}$$

(iii) A combination of the above two examples leads to

$$\langle k'^B; h'^A \mid k^B; h^A\rangle = (k'^B \mid k^B)(h^A \mid \Delta^{-1} \mid h'^A) + \sum_l{}' \sum_{l'}{}' (k'^B \mid l'^A)(l^A \mid k^B)(h^A l'^A \mid \Delta^{-1} \mid l^A h'^A), \tag{3.8}$$

where $(h^A l'^A \mid \Delta^{-1} \mid l^A h'^A)$ is a signed minor of order $N-2$ in Δ_A. Similarly we will find that

(iv) $$\langle k'^B \mid k^B\rangle = (k'^B \mid k^B) - \sum_l \sum_{l'} (k'^B \mid l'^A)(l^A \mid k^B)(l'^A \mid \Delta^{-1} \mid l^A), \tag{3.9}$$

and

(v) $$\langle\ ; h'^A \mid\ ; h^A\rangle = (h^A \mid \Delta^{-1} \mid h'^A). \tag{3.10}$$

The above examples can be extended to a general form as follows:

(vi) $$\langle k_1'^B \cdots k_{m'+n}'^B; h_1'^A \cdots h_{m'}'^A \mid k_1^B \cdots k_{m+n}^B; h_1^A \cdots h_m^A\rangle = \sum_{l_1 \cdots l_{m+n}}{}' \sum_{l'_1 \cdots l'_{m'+n}}{}' [\prod_{j=1}^{m'+n} (k_j'^B \mid l_j'^A) \prod_{i=1}^{m+n} (l_i^A \mid k_i^B)]$$
$$\times (h_1^A \cdots h_m^A l_1'^A \cdots l_{m'}'^A l_{m'+1}'^A \cdots l_{m'+n}'^A \mid \Delta^{-1} \mid l_1^A \cdots l_m^A h_1'^A \cdots h_{m'}'^A l_{m+1}^A \cdots l_{m+n}^A), \tag{3.11}$$

where the summations not only extend over *all distinct indices* $l_1 \cdots l_{m+n}$ or $l_1' \cdots l_{m'+n}'$, but also include terms where

$$(k_j'^B \mid l_j'^A)(l_i^A \mid k_i^B),$$

$$(\cdots h_i^A l_j'^A \cdots \mid \Delta^{-1} \mid \cdots l_i^A h_j'^A \cdots),$$

and

$$(\cdots l_{m+j}'^A \mid \Delta^{-1} \mid \cdots l_{m+i}^A \cdots)$$

are replaced by

$$(k_j'^B \mid k_i^B),$$

$$(\cdots h_i^A \cdots \mid \Delta^{-1} \mid \cdots h_j'^A \cdots),$$

and

$$(\cdots \cdots \mid \Delta^{-1} \mid \cdots \cdots),$$

respectively. Those terms correspond to the first terms in (3.8) and (3.9). After some trivial modification, the expansion (3.11) can be extended to the case where $n<0$ for the calculation of elements of the type (3.2b). The expansion (3.11) is, in fact, a generalization of the Cauchy expansion of a determinant.

In the following, the properties of signed minors $(l_1 \cdots l_m \mid \Delta^{-1} \mid h_1 \cdots h_m)$ will be summarized in the form of two theorems. For simplicity, we shall omit, whenever practical, suffixes A and B, but h and l will always refer to atomic orbitals on $[A]$ and k to those on $[B]$. We note here that the calculation of matrix elements on sublattice $[B]$ can be performed in exactly the same manner as those on $[A]$.

Theorem 1. The cofactor $(l \mid \Delta^{-1} \mid h)$ is the lh element of the inverse of the overlap matrix $\langle \Delta_A \rangle$ whose lh element is given by overlap integral $(l \mid h)$ on sublattice $[A]$. The values of $(l \mid \Delta^{-1} \mid h)$ may be evaluated correctly by using one of the methods discussed in Refs. 13 and 14, even if the values of the overlap integrals are appreciable and the criterion $\sum_{l \neq h} |(l \mid h)| < 1$ is not satisfied.

Since the energy matrix will be eventually expanded in terms of diagrams consisting of $(l \mid h)$ and $(l \mid \Delta^{-1} \mid h)$, we shall represent them, respectively, by a light line and a heavy line starting from point h and ending at point l as is shown in Fig. 1.

The theorem of Jacobi[15] concerning minors of a determinant is useful in the calculation of

$$(l_1 \cdots l_m \mid \Delta^{-1} \mid h_1 \cdots h_m).$$

The theorem can be stated as follows:

Theorem 2. The signed minor $(l_1 \cdots l_m \mid \Delta^{-1} \mid h_1 \cdots h_m)$ is equal to the $m \times m$ determinant whose ij element is given by $(l_i \mid \Delta^{-1} \mid h_j)$:

$$(l_1 \cdots l_m \mid \Delta^{-1} \mid h_1 \cdots h_m)$$
$$= |(l_1 \mid \Delta^{-1} \mid h_1)(l_2 \mid \Delta^{-1} \mid h_2) \cdots (l_m \mid \Delta^{-1} \mid h_m)|. \tag{3.12}$$

Theorem 2 together with the exact calculation of the inverse overlap matrix $(l \mid \Delta^{-1} \mid h)$ on sublattice $[A]$ will yield correct values of $(l_1 \cdots l_m \mid \Delta^{-1} \mid h_1 \cdots h_m)$. It should be noted that the restriction imposed on the summations over $l_1 \cdots l_m$ and $l_1' \cdots l_m'$ in (3.11) can now be removed, since the additional terms generated vanish automatically due to the determinantal structure of $(l_1 \cdots l_m \mid \Delta^{-1} \mid h_1 \cdots h_m)$.

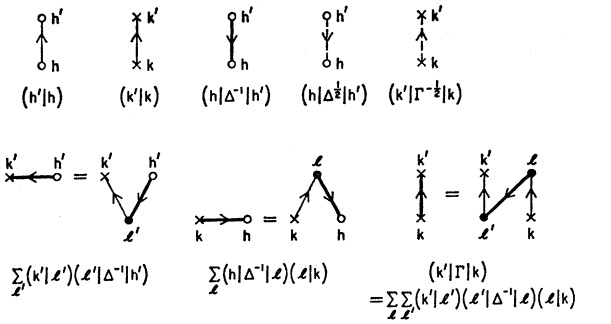

FIG. 1. Summary of the definition of lines used in the diagram representation.

[13] T. Arai and J. R. Gabriel, J. Math. Phys. **8**, 1018 (1967).
[14] J. L. Calais and K. Appel, J. Math. Phys. **5**, 1001 (1964). Also see T. L. Gilbert, *ibid.* **3**, 107 (1962).

[15] See, for instance, A. C. Aitken, *Determinants and Matrices* (Oliver and Boyd, Edinburgh, 1956). The theorem has been used by P.-O. Löwdin, Phys. Rev. **97**, 1474 (1955).

By inserting (3.12) into (3.11), we can expand overlap-matrix elements in terms of overlap integrals $(l \mid h)$ and the inverse matrix elements $(l \mid \Delta^{-1} \mid h)$. The decomposition may be illustrated by diagrams. For example, the expressions (3.8)–(3.10) can be described by Figs. 2(a), 2(b), and 2(c), where a cross (×) denotes an electron which is brought into the subspace G_α from G_β while an open dot represents a hole in G_α. The second and third terms in diagram 2(a) come from the expansion of the 2×2 determinant $(hl' \mid \Delta^{-1} \mid lh')$ in (3.8). Since the restriction on the summations $\sum_{l'} \sum_{\nu'}$ in (3.8) can be removed, it is no longer necessary to indicate l and l' explicitly as distinct points in the diagram. This simplifies the diagrams 2(a) and 2(b) as 2(a′) and 2(b′), where the use of heavy lines is defined in Fig. 1. Let us call a line connecting a cross and a dot a *pair-creation line* and a line connecting two crosses (or two dots) an *electron–electron* (or *hole–hole*) *overlap line*.

Since the values of those lines are independent of other lines in a diagram, they are calculated by the following relations:

(a) the hole–hole overlap line

$$h' \rightarrow h = (h \mid \Delta^{-1} \mid h'), \tag{3.13a}$$

(b) the electron–electron overlap line

$$k \rightarrow k' = (k' \mid \Gamma \mid k) = \sum_{l} \sum_{l'} (k' \mid l')(l' \mid \Delta^{-1} \mid l)(l \mid k), \tag{3.13b}$$

(c) the pair-creation line

$$k \rightarrow h = \sum_{l} (h \mid \Delta^{-1} \mid l)(l \mid k), \tag{3.13c}$$

(d) the pair-creation line

$$h' \rightarrow k' = \sum_{l} (k' \mid l')(l' \mid \Delta^{-1} \mid h'). \tag{3.13d}$$

Figure 3 illustrates diagrams for the general expression (3.11), where 3(a) and 3(b) appear from the diagonal elements of the determinants when $n \geq 0$ and $n \leq 0$, respectively. Those diagrams consist of $m+m'$ creation lines $k_i \rightarrow h_i$ and $h_i' \rightarrow k_i'$, $i=1, 2, \cdots, m$ (or m')

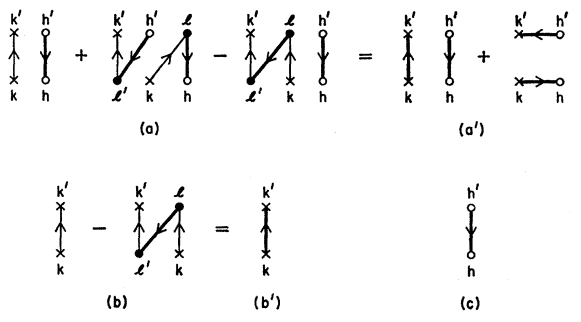

FIG. 2. Expansions of overlap-matrix elements. Diagrams (a) and (a′) are for $\langle k'; h' \mid k; h \rangle$, (b) and (b′) for $\langle k' \mid k \rangle$, and (c) for $\langle\ ; h' \mid\ ; h \rangle$.

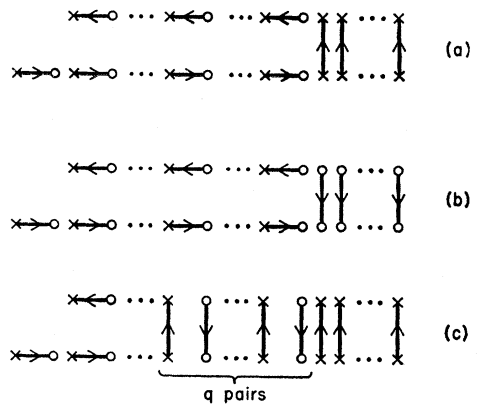

FIG. 3. Diagrams for the general expression of overlap-matrix elements.

and n electron–electron (or hole–hole) overlap lines $k_{m+i} \rightarrow k_{m'+i}'$ (or $h_{m'+i}' \rightarrow h_{m+i}$), $i=1, \cdots, n$. The type of diagrams shown in 3(c) is obtained from 3(a) or 3(b) by the replacement of q pairs of creation lines by q pairs of overlap lines. Other types of diagrams are all generated from those standard diagrams by permutations of upper termini $k_1' \cdots k_{m'+n}'$ and of lower termini $h_1 \cdots h_m$. The permutations are due to the antisymmetrization of the wave functions and introduce sign factors $(-1)^P$ in the resulting diagrams.

IV. ORTHOGONALIZATION AND THE PROJECTED OVERLAP MATRICES

A. Orthogonalization by Projection Operators

To use a perturbation expansion effectively, we need to orthogonalize the basic functions $\mid A \rangle \equiv \mid nmA_p \rangle$ and introduce the concept of quasiparticle states. A set of orthonormal functions obtained by

$$\mid A \rangle_{\text{orth}} \equiv \sum_{A'} \mid A' \rangle [\mathcal{O}^{-1/2}]_{A'A} \tag{4.1}$$

is not convenient to use because the function $\mid A \rangle_{\text{orth}}$ will acquire a large number of unlinked clusters through the inverse overlap matrix $\mathcal{O}^{-1/2}$ even if the original function $\mid A \rangle$ consists of a limited number of clusters. To avoid this complication, we construct an orthonormal set step by step starting from functions $\mid n0A_p \rangle$ of the lowest order in m.

The unperturbed ground-state function $\mid 0A \rangle$ is already normalized in (2.8), while a set of

$$\binom{N}{n}$$

functions

$$\mid n0A_p \rangle, \qquad p=1, 2, \cdots, \binom{N}{n},$$

generated by transposition of n orbitals from G_β to G_α is

orthogonalized as follows:

$$\mathfrak{N}\mid n0A_p\rangle=\sum_q \mid n0A_q\rangle\langle n0A_q\mid \mathcal{O}_{n0}^{-1/2}\mid n0A_p\rangle, \quad (4.2)$$

where by $\langle\cdots\mid \mathcal{O}_{n0}^{-1}\mid\cdots\rangle$ and $\langle\cdots\mid \mathcal{O}_{n0}^{-1/2}\mid\cdots\rangle$ we denote the inverse and the half power of the inverse of the overlap matrix $\langle n0A_q\mid n0A_p\rangle\equiv\langle n0A_q\mid \mathcal{O}_{n0}\mid n0A_p\rangle$ among the

$$\binom{N}{n}$$

functions $\mid n0A_p\rangle$. The meaning of the operator $\mathcal{O}_{n0}\equiv 1$ will become clear shortly. Of course, we need to consider the orthogonalization among functions with a fixed n only; other functions are automatically orthogonal to each other because of their spins.

Wave functions involving single interchanges, $m=1$, are obtained from $\mid n1A_p\rangle$ by projecting out the lower components $\mid 0A\rangle$ or $\mid n0A_p\rangle$ by

$$\mathcal{O}_{n1}\mid n1A_p\rangle=\{1-\mathcal{P}_{n0}\}\mid n1A_p\rangle, \quad (4.3)$$

where the projection operators $\mathcal{O}_{n1}$ and $\mathcal{P}_{n0}$ are defined by

$$\mathcal{P}_{n,0}=\sum_q \mathfrak{N}\mid n0A_q\rangle\langle n0A_q\mid\mathfrak{N}$$
$$=\sum_q\sum_r \mid n0A_q\rangle\langle n0A_q\mid \mathcal{O}_{n0}^{-1}\mid n0A_r\rangle\langle n0A_r\mid, \quad \text{for } n\neq 0, \quad (4.4a)$$

$$\mathcal{P}_0=\mid 0A\rangle\langle 0A\mid, \quad \text{for } n=0, \quad (4.4b)$$

and

$$\mathcal{O}_{n1}=1-\mathcal{P}_{n0}. \quad (4.5)$$

The orthonormal set is then written as

$$\mathfrak{N}\mid n1A_p\rangle=\sum_q \mathcal{O}_{n1}\mid n1A_q\rangle\langle n1A_q\mid \mathcal{O}_{n1}^{-1/2}\mid n1A_p\rangle, \quad (4.6)$$

where $\langle\cdots\mid \mathcal{O}_{nm}^{-1/2}\mid\cdots\rangle$ is the half power of the inverse of the matrix $\langle\cdots\mid \mathcal{O}_{nm}\mid\cdots\rangle$.

Similarly, orthonormal functions with double interchanges are generated from $\mid n2A_p\rangle$ by projecting out the lower components $\mid n0A_q\rangle$ and $\mid n1A_r\rangle$ and then by orthogonalizing the resulting functions $\mathcal{O}_{n2}\mid n2A_p\rangle$. This method can be continued indefinitely. The orthonormal functions $\mathfrak{N}\mid nmA_p\rangle$ with an arbitrary m are given by

$$\mathfrak{N}\mid nmA_p\rangle=\sum_q \mathcal{O}_{nm}\mid nmA_q\rangle\langle nmA_q\mid \mathcal{O}_{nm}^{-1/2}\mid nmA_p\rangle, \quad (4.7)$$

where

$$\mathcal{O}_{nm}\equiv(1-\mathcal{P}_{nm-1})\,\mathcal{O}_{nm-1}, \quad (4.8)$$

and

$$\mathcal{P}_{nm}\equiv\sum_q \mathfrak{N}\mid nmA_q\rangle\langle nmA_q\mid\mathfrak{N}$$
$$=\sum_q\sum_r \mathcal{O}_{nm}\mid nmA_q\rangle$$
$$\times\langle nmA_q\mid \mathcal{O}_{nm}^{-1}\mid nmA_r\rangle\langle nmA_r\mid \mathcal{O}_{nm}. \quad (4.9)$$

A repeated use of the recurrence relation (4.8) for $\mathcal{O}_{nm}$ and the characteristic property of projection operators $\mathcal{P}_{nm}\mathcal{P}_{n'm'}=\mathcal{P}_{nm}\delta_{nn'}\delta_{mm'}$ yield that

$$\mathcal{O}_{nm}=\prod_{i=0}^{m-1}(1-\mathcal{P}_{ni})=1-\sum_{i=0}^{m-1}\mathcal{P}_{ni}; \qquad \mathcal{O}_{n0}=1. \quad (4.10)$$

Also, we find that

$$\mathcal{O}_{nm}\mid nm'\rangle=0, \qquad \text{if } m>m', \quad (4.11)$$

$$\mathcal{P}_{nm}\mid nm'\rangle=0, \qquad \text{if } m>m', \quad (4.12a)$$

and

$$\mathcal{P}_{nm}\mid nm\rangle=\mathfrak{N}\mid nm\rangle, \qquad \text{if } m=m'. \quad (4.12b)$$

In conclusion, the operator $\mathcal{O}_{nm}$ projects out all lower states $\mid nm'A_q\rangle$ where $m'<m$, while $\mathcal{P}_{nm}$ picks up the mth states $\mathfrak{N}\mid nm\rangle$.

B. Expansion of the Projected Overlap Matrices

We shall now apply the expansion method developed in Sec. III to the calculation of the projected overlap matrices $\langle nmA_q\mid \mathcal{O}_{nm}\mid nmA_p\rangle$ and the inverses $\langle nmA_q\mid \mathcal{O}_{nm}^{-1}\mid nmA_p\rangle$ and $\langle nmA_q\mid \mathcal{O}_{nm}^{-1/2}\mid nmA_p\rangle$, which appear in the process of the orthogonalization. We will then find that the operators $\mathcal{O}_{nm}^{\pm l}$ just introduced project out all pair-creation lines and the resulting diagrams for $\langle nmA_q\mid \mathcal{O}_{nm}^{l}\mid nmA_p\rangle$ consist of overlap interaction lines only, where the notation $\langle nmA_q\mid \mathcal{O}_{nm}^{l}\mid nmA_p\rangle$ with $l=1$, -1, and $-\frac{1}{2}$ is used to denote both the overlap matrix and the inverses.

For example, use of the relation $\mathcal{O}_{01}=1-\mathcal{P}_0$ and $\mathcal{P}_0\equiv\mid 0\rangle\langle 0\mid$ leads to

$$\langle k';h'\mid \mathcal{O}_{01}\mid k;h\rangle=\langle k';h'\mid k;h\rangle-\langle k';h'\mid 0\rangle\langle 0\mid k;h\rangle. \quad (4.13)$$

The first term on the right, $\langle k';h'\mid k;h\rangle$, is given by the sum of two diagrams in Fig. 2(a′), but $\langle k';h'\mid 0\rangle\times\langle 0\mid k;h\rangle$ is equal to the second diagram alone. Hence, only the overlapping pair diagram contributes to $\langle k';h'\mid \mathcal{O}_{01}\mid k;h\rangle$, yielding that

$$\langle k';h'\mid \mathcal{O}_{01}\mid k;h\rangle=(k'\mid\Gamma\mid k)\,(h\mid\Delta^{-1}\mid h'). \quad (4.14a)$$

Here the complete cancellation of the second diagram results from the fact that the two lines in the diagram are independent of each other due to the determinantal structure of $\langle k';h'\mid k;h\rangle$. The inverses $\langle k';h'\mid \mathcal{O}_{01}^{l}\mid k;h\rangle$, where $l=-1$ and $-\frac{1}{2}$, are also given by

$$\langle k';h'\mid \mathcal{O}_{01}^{l}\mid k;h\rangle=(k'\mid\Gamma^{l}\mid k)\,(h\mid\Delta^{-l}\mid h'), \quad (4.14b)$$

as is proved by appropriate matrix multiplications, where $(h\mid\Delta\mid h')\equiv(h\mid h')$.

The values of matrix elements $(k'\mid\Gamma^{l}\mid k)$ and $(h\mid\Delta^{-l}\mid h')$, for $l=\pm 1$ and $-\frac{1}{2}$, which appear in the expressions in (4.14) are evaluated as follows. The inverse $(h\mid\Delta^{-1}\mid h')$ can be evaluated accurately by Theorem 1. Use of the results in (3.13b) will yield the value of $(k'\mid\Gamma\mid k)$. Let $\langle\Gamma\rangle$ be the matrix whose

$k'k$ element is given by $(k' \mid \Gamma \mid k)$. Since $(k' \mid \Gamma \mid k)$ behaves similar to the overlap integral $(k' \mid k)$, we can compute the inverse $(k' \mid \Gamma^{-1} \mid k)$ of the matrix $\langle\Gamma\rangle$ equally well by one of the methods used in the calculation of the inverse overlap matrix $\langle\Delta^{-1}\rangle$.

Quantities like $(h \mid \Delta^{\pm 1/2} \mid h')$ and $(k' \mid \Gamma^{\pm 1/2} \mid k)$ are calculated by a similar method. If, for instance, we truncate the matrices Δ and Γ, the eigenvalues $(1+\lambda)$ and $(1+\lambda_\Gamma)$ can be evaluated, and the desired quantities will be obtained, by $\Delta^{\pm 1/2}=U^\dagger(1+\lambda)^{\pm 1/2}U$ and $\Gamma^{\pm 1/2}=U_\Gamma{}^\dagger(1+\lambda_\Gamma)^{\pm 1/2}U_\Gamma$. The accuracy of the calculation may be improved by the expansion technique discussed in Ref. 13.

Since it is possible to expand $(h \mid \Delta^{1/2} \mid h')$ and $(k' \mid \Gamma^{-1/2} \mid k)$ in terms of $(h \mid h')$ and $(k' \mid \Gamma \mid k)$, respectively, any of them can be written as a sum of linked diagrams composed of light lines representing the overlap integral $(h \mid h')$ or heavy lines describing $(k' \mid \Gamma \mid k)$. This shows that the two termini $h'h$ or kk' involved are linked. Let us denote the linkage by a broken line connecting the two points as is shown in Fig. 1, and call them (inverse) overlap lines.

The decomposition procedure can be extended to matrices $\langle nmA_q \mid \mathcal{O}_{nm}{}^l \mid nmA_p\rangle$ of higher order. The result may be summarized as follows:

Theorem 3. All pair-creation lines in

$$\langle nmA_q \mid \mathcal{O}_{nm}{}^l \mid nmA_p\rangle$$

are projected out by the operators $\mathcal{O}_{nm}{}^l$ and hence the only lines in the diagrams remaining are $2m+n$ overlap lines. Those diagrams are all generated from a standard diagram by permutations of the upper termini of the overlap lines between electrons as well as by permutations of the lower termini of the overlap lines between holes. Hence

$$\langle k_1'\cdots k_{m+n}';\, h_1'\cdots h_m' \mid \mathcal{O}_{nm}{}^l \mid k_1\cdots k_{m+n};\, h_1\cdots h_m\rangle$$
$$= D_{nm}{}^l \sum_P \sum_Q (-1)^{P+Q} \prod_{i=1}^{m+n} \prod_{j=1}^{m} \times (k_{P_i}' \mid \Gamma^l \mid k_i)(h_j \mid \Delta^{-l} \mid h_{Q_j}'), \quad (4.15)$$

and a similar expression for $\langle\cdots\mid \mathcal{O}_{-nm}{}^l \mid\cdots\rangle$, where

$$D_{\mid n\mid m}{}^l = 1, \qquad \text{for } l=1, \quad (4.16a)$$

$$D_{\mid n\mid m}{}^l = \{(m+\mid n\mid)!\, m!\}^{-1}, \quad \text{for } l=-1 \text{ or } -\tfrac{1}{2}, \quad (4.16b)$$

and $P_1\cdots P_m$ denotes the series generated from $1, 2, \cdots, m$ by a permutation P while the summation $\sum_P$ includes all possible permutations. The normalization coefficient $D_{nm}{}^l$ given by (4.16) is a consequence of the definition of $(\cdots\mid \Delta^{-1} \mid\cdots)$ as given by (3.11).

The theorem will be proved in the following. Since $\mathcal{O}_{n0}$ is equal to unity, $\langle k_1'\cdots k_n' \mid \mathcal{O}_{n0} \mid k_1\cdots k_n\rangle$ is simply given by (3.11), that is,

$$\langle k_1'\cdots k_n' \mid \mathcal{O}_{n0} \mid k_1\cdots k_n\rangle = \sum_{l_1\cdots l_n} \sum_{l_1'\cdots l_1'} \{\prod_{i=1}^{n} (k_i' \mid l_i')(l_i \mid k_i)\} \times (l_1'\cdots l_n' \mid \Delta^{-1} \mid l_1\cdots l_n), \quad (4.17)$$

where the summation $\sum_{l_1\cdots l_n}$ includes, as before, terms obtained by the replacement of $(k_j' \mid l_j')(l_i \mid k_i)$ and $(\cdots l_j'\cdots \mid \Delta^{-1} \mid \cdots l_i\cdots)$ by $(k_j' \mid k_i)$ and $(\cdots\ \cdots \mid \Delta^{-1} \mid \cdots\ \cdots)$. Use of (3.12) and (3.13b) in (4.17) will yield that

$$\langle k_1'\cdots k_n' \mid \mathcal{O}_{n0} \mid k_1\cdots k_n\rangle = \sum_P (-1)^P \prod_{i=1}^{n} (k_{P_i}' \mid \Gamma \mid k_i), \quad (4.18a)$$

which proves (4.15) for $\mathcal{O}_{n0}$. The inverse is also given by

$$\langle k_1'\cdots k_n' \mid \mathcal{O}_{n0}{}^{-l} \mid k_1\cdots k_n\rangle = (n!)^{-1} \sum_P (-1)^P \prod_{i=1}^{n} (k_{P_i}' \mid \Gamma^{-l} \mid k_i). \quad (4.18b)$$

This is proved by appropriate matrix multiplications. For instance, use of the expressions on the right of (4.18) in

$$\sum_{\bar{k}_1\cdots\bar{k}_n} \langle k_1'\cdots k_n' \mid \mathcal{O}_{n0}{}^{-1} \mid \bar{k}_1\cdots\bar{k}_n\rangle\langle\bar{k}_1\cdots\bar{k}_n \mid \mathcal{O}_{n0} \mid k_1\cdots k_n\rangle \quad (4.19)$$

will yield the desired δ function, because the summation $\sum_{\bar{k}_1\cdots\bar{k}_n}$ can be replaced by a set of unrestricted summations $(1/n!)\sum_{\bar{k}_1}\cdots\sum_{\bar{k}_n}$. The expressions in (4.18) illustrate that diagrams for $\langle k_1'\cdots k_n' \mid \mathcal{O}_{n0}{}^l \mid k_1\cdots k_n\rangle$ consists of nothing but n overlap lines. Thus, the theorem is shown to be valid for $\mathcal{O}_{n0}{}^l$.

More generally, it will be found from (3.11) that $\langle k_1'\cdots k_{m'+n}';\, h_1'\cdots h_{m'}' \mid \mathcal{O}_{n0} \mid k_1\cdots k_{m+n};\, h_1\cdots h_m\rangle$ involves at least n overlap lines which connect k and k'; the remaining $m+m'$ pairs of termini may contribute in forming either pair-creation or overlap lines, thus yielding an overlap matrix not involving any projection operators $\mathcal{O}$. Therefore, $\langle\cdots\mid \mathcal{O}_{n0} \mid\cdots\rangle$ may be decomposed as follows:

$$\langle k_1'\cdots k_{m'+n}';\, h_1'\cdots h_{m'}' \mid \mathcal{O}_{n0} \mid k_1\cdots k_{m+n};\, h_1\cdots h_m\rangle$$
$$= \sum_{(P)} \sum_{(Q)} \langle k_{Q_1}'\cdots k_{Q_n}' \mid \mathcal{O}_{n0} \mid k_{P_1}\cdots k_{P_n}\rangle\langle k_{Q_{n+1}}'\cdots k_{Q_{n+m}}';\, h_1'\cdots h_{m'}' \mid k_{P_{n+1}}\cdots k_{P_{n+m}};\, h_1\cdots h_m\rangle$$
$$= \sum_{(P)} \sum_{(Q)} \langle n0A_{q_n} \mid \mathcal{O}_{n0} \mid n0A_{p_n}\rangle\langle 0m'A_{q_0} \mid 0mA_{p_0}\rangle, \quad (4.20)$$

where two series of numbers $P_1\cdots P_n$ and $P_{n+1}\cdots P_{n+m}$ result from a partition of $1, 2, \cdots, m+n$ into two parts;

one part contains n and the other m numbers. The summation $\sum_{(P)}$ includes

$$\binom{n+m}{n}$$

distinct partitions of this kind.

The same arguments will be applied to the decomposition of $\langle\cdots|\ \mathcal{O}_{-n0}{}^{l}\ |\cdots\rangle$, and we will find at least n overlap lines connecting $h'h$ pairs of holes.

The expansion of $\langle nm''A_q\ |\ \mathcal{O}_{n1}\ |\ nm'A_p\rangle$, for arbitrary n, m', and m'', may be performed similarly to that of $\langle\cdots|\ \mathcal{O}_{01}\ |\cdots\rangle$, as is illustrated in (4.13) and (4.14). It will then be found that a nonvanishing contribution to $\langle\cdots|\ \mathcal{O}_{n1}\ |\cdots\rangle$ appears only if one more pair of electron-electron and hole-hole overlap lines connect $\langle\cdots|$ to $|\cdots\rangle$ in addition to the n overlap lines already found in the expansion of $\langle\cdots|\ \mathcal{O}_{n0}\ |\cdots\rangle$.

The calculation can be extended to higher-order terms. To prove the expansion for an arbitrary m by an induction method, we first assume that

$$\langle nm''A_q\ |\ \mathcal{O}_{nm}\ |\ nm'A_p\rangle \quad \text{with} \quad m', m''\geq m,$$

involves at least $2m+n$ overlap lines which connect $\langle\cdots|$ to $|\cdots\rangle$ and show that the statement is also true when m is replaced by $m+1$.

The original assumption implies that

$$\langle nmA_q\ |\ \mathcal{O}_{nm}{}^{l}\ |\ nmA_p\rangle, \quad \text{for} \quad l=\pm 1 \text{ or } -\tfrac{1}{2},$$

is written as (4.15). Furthermore, since the $2m+n$ lines are disconnected from the remainder in

$$\langle nm''A_q\ |\ \mathcal{O}_{nm}\ |\ nm'A_p\rangle,$$

we can separate them as follows:

$$\begin{aligned}\langle nm''A_q\ |\ \mathcal{O}_{nm}\ |\ nm'A_p\rangle&\\ =\sum_{(P)}\sum_{(Q)}&\langle 0\ m''-m\ A_{q0}\ |\ 0\ m'-m\ A_{p0}\rangle\\ &\times\langle nmA_{q_n}\ |\ \mathcal{O}_{nm}\ |\ nmA_{p_n}\rangle,\end{aligned}\tag{4.21}$$

where the summation $\sum_{(P)}$ includes

$$\binom{m'+n}{m+n}\binom{m'}{m}$$

distinct terms generated by appropriate partitions of indices $k_1\cdots k_{m'+n}h_1\cdots h_{m'}$ into two parts.

Use of (4.8) yields the expansion of $\langle\cdots|\ \mathcal{O}_{nm+1}\ |\cdots\rangle$:

$$\begin{aligned}&\langle nm''A_q\ |\ \mathcal{O}_{nm+1}\ |\ nm'A_p\rangle\\ &=\langle nm''A_q\ |\ \mathcal{O}_{nm}\ |\ nm'A_p\rangle-\sum_{\bar{p}}\sum_{\bar{q}}\langle nm''A_q\ |\ \mathcal{O}_{nm}\ |\ nmA_{\bar{q}}\rangle\\ &\times\langle nmA_{\bar{q}}\ |\ \mathcal{O}_{nm}{}^{-1}\ |\ nmA_{\bar{p}}\rangle\langle nmA_{\bar{p}}\ |\ \mathcal{O}_{nm}\ |\ nm'A_p\rangle,\end{aligned}\tag{4.22}$$

where the first and second terms on the right can be divided into two by (4.21). In particular, the second term will become

$$\begin{aligned}-\sum_{(P)}\sum_{(Q)}\sum_{\bar{p}}\sum_{\bar{q}}&\langle 0\ m''-m\ A_{q0}\ |\ 0\rangle\\ &\times\langle nmA_{q_n}\ |\ \mathcal{O}_{nm}\ |\ nmA_{\bar{q}}\rangle\\ &\times\langle nmA_{\bar{q}}\ |\ \mathcal{O}_{nm}{}^{-1}\ |\ nmA_{\bar{p}}\rangle\\ &\times\langle nmA_{\bar{p}}\ |\ \mathcal{O}_{nm}\ |\ nmA_{p_n}\rangle\\ &\times\langle 0\ |\ 0\ m'-m\ A_{p0}\rangle\\ =-\sum_{(P)}\sum_{(Q)}&\langle 0\ m''-m\ A_{q0}\ |\ 0\rangle\\ &\times\langle nmA_{q_n}\ |\ \mathcal{O}_{nm}\ |\ nmA_{p_n}\rangle\\ &\times\langle 0\ |\ 0\ m'-m\ A_{p0}\rangle.\end{aligned}\tag{4.23}$$

Hence the expression (4.22) may be written in the form

$$\begin{aligned}&\langle nm''A_q\ |\ \mathcal{O}_{nm+1}\ |\ nm'A_p\rangle\\ &=\sum_{(P)}\sum_{(Q)}\{\langle 0\ m''-m\ A_{q0}\ |\ 0\ m'-m\ A_{p0}\rangle\\ &-\langle 0\ m''-m\ A_{q0}\ |\ 0\rangle\langle 0\ |\ 0\ m'-m\ A_{p0}\rangle\}\\ &\times\langle nmA_{q_n}\ |\ \mathcal{O}_{nm}\ |\ nmA_{p_n}\rangle.\end{aligned}\tag{4.24}$$

The quantity in $\{\ \}$ on the right of (4.24) is equivalent to the expression on the right of (4.13). Hence the expression on the right of (4.24) vanishes unless one more pair of overlap lines connects $\langle\cdots|$ to $|\cdots\rangle$ in addition to the $2m+n$ lines which already exist in $\langle\cdots|\ \mathcal{O}_{nm}\ |\cdots\rangle$. This proves the original assumption as well as Theorem 3 and $\langle nmA_q\ |\ \mathcal{O}_{nm}{}^{l}\ |\ nmA_p\rangle$ is written as (4.15). The expression for the inverses is proved immediately by appropriate matrix multiplications of the type (4.19). We note that $\langle nm''A_q\ |\ \mathcal{O}_{nm}{}^{l}\ |\ nm'A_p\rangle=0$ if m' or m'' is less than m, because of (4.11).

V. EXPANSION OF THE PROJECTED INTERACTION MATRICES

A. Separation of the Hamiltonian

In this section, we shall calculate the projected interaction matrices $\langle n'm'p'\ |\ \mathcal{O}_{n'm'}\mathcal{H}\mathcal{O}_{nm}\ |\ nmp\rangle$ by the technique developed in Secs. III and IV. The projection operator used here is considered to operate in both subspaces G_α and G_β simultaneously as follows:

$$\mathcal{O}_{nm}\ |\ nmp\rangle\equiv\mathcal{O}_{nm}\ |\ nmA_p\rangle\ \mathcal{O}_{-nm}\ |\ -nmB_p\rangle,\tag{5.1}$$

while the Hamiltonian $\mathcal{H}$ is assumed to be of the form:

$$\begin{aligned}\mathcal{H}=\sum_{j}^{2N}\mathcal{H}^{(1)}(\boldsymbol{r}_j)+\sum_{j1>j2}^{2N}\sum^{2N}\mathcal{H}^{(2)}(\boldsymbol{r}_{j_1},\boldsymbol{r}_{j_2})&\\ +\sum_{j1>j2}^{2N}\sum^{2N}|R_{j_1}-R_{j_2}|^{-1},&\end{aligned}\tag{5.2}$$

where j illustrates a site in both sublattices $[A]$ and $[B]$ and the summation $\sum_j{}^{2N}$ is equivalent to $\sum_{h=1}{}^{N}+\sum_{k=1}{}^{N}$.

For simplicity, $\mathcal{H}$ is considered to be a function of positional coordinates only, although the method can be extended to the case where $\mathcal{H}$ involves spin variables. The number of electrons in a subspace is then a constant $N\pm n$, and nonvanishing matrix elements appear only if $n=n'$. Consequently, we only need to calculate elements of the form $\langle nm'p' \mid \mathcal{O}_{nm'}\mathcal{H}\mathcal{O}_{nm} \mid nmp\rangle$ which can be divided into two parts as follows:

$$\langle nm'p' \mid \mathcal{O}_{nm'}\mathcal{H}\mathcal{O}_{nm} \mid nmp\rangle = \sum_{\alpha\beta}\langle nm'A_{p'} \mid \mathcal{O}_{nm'}\mathcal{H}_\alpha\mathcal{O}_{nm} \mid nmA_p\rangle \times\langle -nm'B_{p'} \mid \mathcal{O}_{-nm'}\mathcal{H}_\beta\mathcal{O}_{-nm} \mid -nmB_p\rangle. \quad (5.3)$$

The Hamiltonian $\mathcal{H}_\alpha$ involves only $N+n$ variables belonging to G_α. The other $N-n$ variables do not appear in G_α; they behave like parameters in $\langle\cdots\mathcal{H}_\alpha\cdots\rangle$ and should be transferred to the second integral $\langle\cdots\mathcal{H}_\beta\cdots\rangle$.

If, for instance, $\mathcal{H}_\alpha$ is

$$\mathcal{H}_\alpha \Rightarrow \sum_j^{G\alpha}\mathcal{H}^{(1)}(\boldsymbol{r}_j)+\sum_{j_1>j_2}^{G\alpha}\sum^{G\alpha}\mathcal{H}^{(2)}(\boldsymbol{r}_{j_1},\boldsymbol{r}_{j_2}) +\sum_{j_1>j_2}^{G\alpha}\sum^{G\alpha}\mid R_{j_1}-R_{j_2}\mid^{-1}, \quad (5.4a)$$

then $\mathcal{H}_\beta$ is equal to unity and vice versa. The two-body interactions between G_α and G_β are formally partitioned into $\mathcal{H}_\alpha$ and $\mathcal{H}_\beta$ as follows:

$$\mathcal{H}_\alpha \Rightarrow \sum_j^{G\alpha}\sum_{j_2}^{G\beta}\langle -nm'B_{p'} \mid \mathcal{O}_{-nm'}\mathcal{H}^{(2)}(\boldsymbol{r}_j,\boldsymbol{r}_{j_2})\,\mathcal{O}_{-nm} \mid -nmB_p\rangle_{r_j=\text{const}}, \quad (5.4b)$$

and

$$\mathcal{H}_\beta = \sum_j^{G\beta}\sum_{j_1}^{G\alpha}\langle nm'A_{p'} \mid \mathcal{O}_{nm'}\mathcal{H}^{(2)}(\boldsymbol{r}_j,\boldsymbol{r}_{j_1})\,\mathcal{O}_{nm} \mid nmA_p\rangle_{r_j=\text{const}}. \quad (5.4c)$$

By $\mathcal{H}_{\alpha\mathrm{I}}$ and $\mathcal{H}_{\alpha\mathrm{II}}$, we denote one- and two-body interaction parts of $\mathcal{H}_\alpha$.

B. Expansion of the Interaction Matrices

We shall now demonstrate the expansions of the interaction matrices by simple examples. For instance, use of expansions like (3.4) in $\langle 0A \mid \mathcal{H}_\alpha \mid 0A\rangle$ yields that

$$\langle 0A \mid \mathcal{H}_{\alpha\mathrm{I}} \mid 0A\rangle = \sum_{h=1}^{N}\sum_{l=1}^{N}(l\mid\mathcal{H}(\boldsymbol{r})\mid h)(h\mid\Delta^{-1}\mid l), \quad (5.5a)$$

and

$$\langle 0A \mid \mathcal{H}_{\alpha\mathrm{II}} \mid 0A\rangle = \sum_{h_1=1}^{N}\sum_{h_2=1}^{N}\sum_{l_1=1}^{N}\sum_{l_2=1}^{N}(l_1l_2\mid\mathcal{H}^{(2)}(\boldsymbol{r}_1\boldsymbol{r}_2)\mid h_1h_2) \times(h_1h_2\mid\Delta^{-1}\mid l_1l_2), \quad (5.5b)$$

where $\mathcal{H}(\boldsymbol{r})$ may be either the one-body potential $\mathcal{H}^{(1)}(\boldsymbol{r})$ in (5.4a) or the projection of the two-body interaction onto the G_α space as defined by (5.4b). We shall illustrate the expansions by diagrams in Fig. 4, where wavy lines represent the dynamical interactions $(l\mid\mathcal{H}(\boldsymbol{r})\mid h)$ and $(l_1l_2\mid\mathcal{H}^{(2)}(\boldsymbol{r}_1\boldsymbol{r}_2)\mid h_1h_2)$. A solid dot assumes the sum over all sites in the lattice. We note that those diagrams do not carry open dots and crosses which would otherwise appear in one of the wave functions. Consequently, this type of interaction cannot propagate to other matrices in the course of a perturbation expansion, and their contributions are limited to the *self-energy* of the matrix.

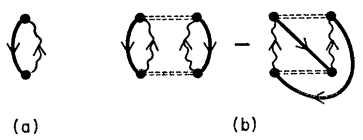

FIG. 4. Self-energy diagrams; (a) is for $\langle 0A \mid \mathcal{H}_{\alpha\mathrm{I}} \mid 0A\rangle$ and (b) for $\langle 0A \mid \mathcal{H}_{\alpha\mathrm{II}} \mid 0A\rangle$.

The matrix element $\langle k';\, h' \mid \mathcal{H}_{\alpha\mathrm{I}} \mid k;\, h\rangle$ is expanded as[16]

$$\begin{aligned}\langle k';\, h' \mid \mathcal{H}_{\alpha\mathrm{I}} \mid k;\, h\rangle &= (k' \mid \mathcal{H}(\boldsymbol{r}_h)\mid k)(h\mid\Delta^{-1}\mid h') \\ &+\sum_l\sum_{l'}\{(k'\mid\mathcal{H}(\boldsymbol{r}_{l'})\mid l')(l\mid k)(hl'\mid\Delta^{-1}\mid lh') \\ &+(l\mid\mathcal{H}(\boldsymbol{r}_h)\mid k)(k'\mid l')(hl'\mid\Delta^{-1}\mid lh')\} \\ &+\sum_{h''}\sum_{l''}(l''\mid\mathcal{H}(\boldsymbol{r}_{h''})\mid h'')(k'\mid k)(hh''\mid\Delta^{-1}\mid h'l'') \\ &+\sum_{h''}\sum_{l''}\sum_l\sum_{l'}(l''\mid\mathcal{H}(\boldsymbol{r}_{h''})\mid h'')(k'\mid l') \\ &\times(l\mid k)(hl'h''\mid\Delta^{-1}\mid lh'l''). \end{aligned} \quad (5.6)$$

A similar series may be found for $\langle k';\, h' \mid \mathcal{H}_{\alpha\mathrm{II}} \mid k;\, h\rangle$. The expansion (5.6) is represented by diagrams in

[16] Expansions like (5.5) and (5.6) may be obtained easily if the permutation operator $\Sigma_P(-1)^P P$ involved in the wave function on the right $\mid\cdots\rangle$ is transferred to the left, $\langle\cdots\mid$. The matrix element is then written as

$$\langle\cdots\mid\mathcal{H}\mid\cdots\rangle = C^{-1}\sum_P(-1)^P \times\int\{P_r\Phi'(1,2,\cdots,2N)\,P_s\Theta'(1,2,\cdots,2N)\}^* \times\mathcal{H}\Phi(1,2,\cdots,2N)\Theta(1,2,\cdots,2N)\,d\tau,$$

and electron h in $\Phi(1,2,\cdots,2N)\Theta(1,2,\cdots,2N)$ occupies a fixed orbital h (or k). More detailed manipulation will be found in Ref. 4.

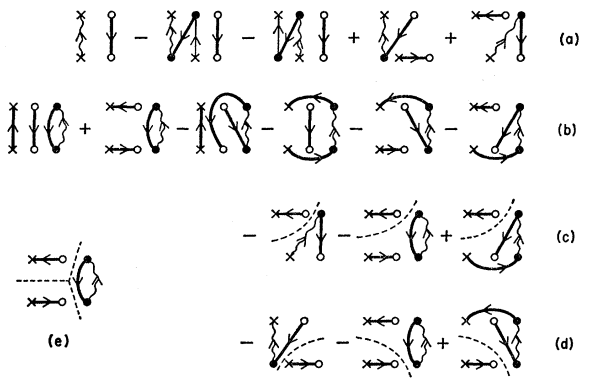

FIG. 5. Diagrams for $\langle k';\, h' \mid \mathcal{O}_{01}\mathcal{H}_{\alpha I}\mathcal{O}_{01} \mid k;\, h\rangle$; (a) and (b) are for $\langle k';\, h' \mid \mathcal{H}_{\alpha I} \mid k;\, h\rangle$, (c) for $\langle k';\, h';\, 0\rangle\langle 0 \mid \mathcal{H}_{\alpha I} \mid k;\, h\rangle$, (d) for $\langle k';\, h' \mid \mathcal{H}_{\alpha I} \mid 0\rangle\langle 0 \mid k;\, h\rangle$, and (e) for

$$\langle k';\, h' \mid 0\rangle\langle 0 \mid \mathcal{H}_{\alpha I} \mid 0\rangle\langle 0 \mid k;\, h\rangle.$$

Figs. 5(a) and 5(b). We may classify those diagrams into three groups as follows.

The first group consists of the first two diagrams in 5(b) and is derived from the third and fourth terms in (5.6). They are superpositions of two disconnected parts; the diagrams for the overlap matrix $\langle k';\, h' \mid k;\, h\rangle$ and a self-energy diagram. The last four diagrams in 5(b) form the second group. They are generated from the diagrams in the first group by interchanges of termini of heavy lines belonging to the self-energy and overlap parts, and may be called *kinematical-interaction* diagrams. The last group is derived from the first and second terms in (5.6). It is generated from the diagrams for $\langle k';\, h' \mid k;\, h\rangle$ by replacing one of the light lines making up the heavy lines by an interaction line. They may be called *dynamical-interaction* diagrams.

The method is readily extended to the calculation of any interaction matrix element and the diagrams may be generated by the following prescriptions.

(a) Draw all diagrams necessary to describe the overlap-matrix element $\langle\cdots|\cdots\rangle$ and add a self-energy diagram to each of them. Here crosses and open dots are fixed points specified in the wave functions $\langle\cdots|$ and $|\cdots\rangle$ but solid dots involved in the self-energy part represent the sum over all sites in the sublattice excluding those points already occupied by open dots. This creates all diagrams belonging to the first group.

(b) Construct all possible kinematical-interaction diagrams by connecting one or two pair-creation or overlap lines to the self-energy part by interchanges of the termini. This generates all diagrams in the second group.

(c) When a solid dot in a self-energy diagram overlaps with an open dot, that portion of the diagram is replaced by a dynamical-interaction diagram. This yields the diagrams in the third group.

Let us call a portion of a diagram a *linked interaction part* if all its points are connected with each other and if it contains an interaction line. The rest of the diagram may be referred to as a *normalization part.*

C. Expansion of the Projected Interaction Matrices

Projected interaction matrices

$$\langle nm'A_{p'} \mid \mathcal{O}_{nm'}\mathcal{H}_{\alpha}\mathcal{O}_{nm} \mid nmA_{p}\rangle$$

may be expanded similarly. Since the operators $\mathcal{O}_{nm}$ and $\mathcal{O}_{nm'}$ project out pair-creation lines and $\mathcal{H}_{\alpha}$ interacts with only a few lines, it is expected that diagrams for a projected interaction matrix element will be superpositions of diagrams of projected overlap-matrix elements and self-energy, dynamical-interaction or kinematical-interaction diagrams. Let us illustrate this by simple examples.

(1) Since $\mathcal{O}_{\pm 10}=1$, the expansions of

$$\langle \pm 1\ 0\ A \mid \mathcal{O}_{\pm 10}\mathcal{H}_{\alpha}\mathcal{O}_{\pm 10} \mid \pm 1\ 0A\rangle$$

may be carried out by the prescriptions (a)$\sim$(c). The results are summarized in Fig. 6, where each solid dot represents the sum over-all sites excluding points already occupied by other dots.

(ii) Use of the relation

$$\mathcal{O}_{01}=1-|\,0\rangle\langle 0\,| \quad \text{in} \quad \langle 0 \mid \mathcal{H}_{\alpha}\mathcal{O}_{01} \mid 01A\rangle$$

will yield that

$$\langle 0 \mid \mathcal{H}_{\alpha}\mathcal{O}_{01} \mid k;\, h\rangle=\langle 0 \mid \mathcal{H}_{\alpha} \mid k;\, h\rangle-\langle 0 \mid \mathcal{H}_{\alpha} \mid 0\rangle\langle 0 \mid k;\, h\rangle. \tag{5.7}$$

Figure 7 illustrates Eq. (5.7), where the first three diagrams in the first line result from the first term in (5.7) and the last one from the second term. The dotted line indicates that the two parts in the last diagram are independent of each other and, hence, the solid dot in the lower terminal is allowed to overlap with the open dot, while this is not permitted in the second diagram. Consequently, the cancellation of these two diagrams is not complete and the difference is given by the diagram shown in the middle of the second line. We shall call this a *cumulant-correction* diagram. The

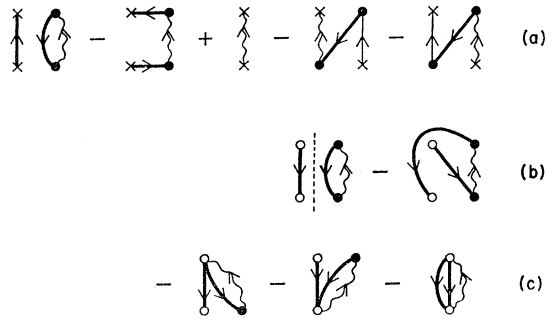

FIG. 6. Diagrams for $\langle \pm 10A \mid \mathcal{O}_{\pm 10}\mathcal{H}_{\alpha I}\mathcal{O}_{\pm 10} \mid \pm 10A\rangle$; (a) is for $\langle 10A \mid \mathcal{O}_{10}\mathcal{H}_{\alpha I}\mathcal{O}_{10} \mid 10A\rangle$ and (b) and (c) are for

$$\langle -10A \mid \mathcal{O}_{-10}\mathcal{H}_{\alpha I}\mathcal{O}_{-10} \mid -10A\rangle.$$

complete expression of $\langle 0 \mid \mathcal{H}_\alpha \mathcal{O}_{01} \mid k; h\rangle$ is given by the three diagrams in the second line. Diagrams for $\langle 0 \mid \mathcal{H}_{\alpha\mathrm{II}} \mathcal{O}_{01} \mid k; h\rangle$ may be generated by appropriate replacements of interaction lines.

(iii) The method can be extended to the expansion of $\langle k'; h' \mid \mathcal{O}_{01}\mathcal{H}_{\alpha\mathrm{I}}\mathcal{O}_{01} \mid k; h\rangle$, as follows:

$$\begin{aligned}\langle k'; h' \mid \mathcal{O}_{01}\mathcal{H}_{\alpha\mathrm{I}}\mathcal{O}_{01} \mid k; h\rangle &= \langle k'; h' \mid \mathcal{H}_{\alpha\mathrm{I}} \mid k; h\rangle \\ &- \langle k'; h' \mid 0\rangle\langle 0 \mid \mathcal{H}_{\alpha\mathrm{I}} \mid k; h\rangle - \langle k'; h' \mid \mathcal{H}_{\alpha\mathrm{I}} \mid 0\rangle\langle 0 \mid k; h\rangle \\ &+ \langle k'; h' \mid 0\rangle\langle 0 \mid \mathcal{H}_{\alpha\mathrm{I}} \mid 0\rangle\langle 0 \mid k; h\rangle. \quad (5.8)\end{aligned}$$

Diagrams for each term on the right of (5.8) are listed separately in Fig. 5. Here diagrams involving an isolated pair-creation line will cancel each other, but again the cancellation is not complete, leaving cumulant-correction diagrams as the remainder. For instance, the first diagram in 5(c) is equal to the last diagram in 5(a) plus the first diagram in the second row in Fig. 8. The complete sum is illustrated in Fig. 8, where the diagrams in the second row are all cumulant-correction diagrams. We note that all points in the diagrams in Fig. 8 are now distinct.

The expansion may be extended to more complicated elements, but we can by analogy expect that pair-creation lines are either projected out by operators $\mathcal{O}_{nm}$ or connected to the linked interaction part by the *interchange mechanism* described in the prescription (b) or by the *cumulative overlapping mechanism* just discussed. We shall prove this in the following. Since $\mathcal{O}_{n0}=1$, the prescriptions (a)$\sim$(c) are directly applicable to the calculation of $\langle nm''A \mid \mathcal{O}_{n0}\mathcal{H}_\alpha\mathcal{O}_{n0} \mid nm'A\rangle$, and it will be found that at least n lines should connect the lower termini to the upper termini in order to find a nonvanishing contribution. Of course, any one of them could include an interaction line. The quantity $\langle\cdots|\cdots\mathcal{H}_{\alpha\mathrm{I}}\mathcal{O}_{n1} \mid nm'A_p\rangle$ may be expanded as

$$\begin{aligned}\langle\cdots|\cdots\mathcal{H}_{\alpha\mathrm{I}}\mathcal{O}_{n1} \mid nm'A_p\rangle &= \langle\cdots|\cdots\mathcal{H}_{\alpha\mathrm{I}}\mathcal{O}_{n0} \mid nm'A_p\rangle \\ &- \sum_{\bar{q}}\sum_{\bar{q}'}\langle\cdots|\cdots\mathcal{H}_{\alpha\mathrm{I}}\mathcal{O}_{n0} \mid n0A_{\bar{q}}\rangle \\ &\times\langle n0A_{\bar{q}} \mid \mathcal{O}_{n0}^{-1} \mid n0A_{\bar{q}'}\rangle \\ &\times\langle n0A_{\bar{q}'} \mid \mathcal{O}_{n0} \mid nm'A_p\rangle. \quad (5.9)\end{aligned}$$

Use of a decomposition similar to (4.21) and (4.23) on the right of (5.9) yields that

$$\begin{aligned}\langle\cdots|\cdots\mathcal{H}_{\alpha\mathrm{I}}\mathcal{O}_{n1} \mid nm'A_p\rangle &= \langle\cdots|\cdots\mathcal{H}_{\alpha\mathrm{I}}\mathcal{O}_{n0} \mid nm'A_p\rangle \\ &- \langle\cdots|\cdots\mathcal{H}_{\alpha\mathrm{I}}\mathcal{O}_{n0} \mid n0A_{p_n}\rangle\langle 0A \mid 0m'A_{p_0}\rangle. \quad (5.10)\end{aligned}$$

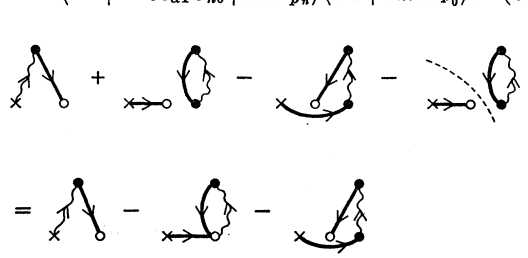

FIG. 7. Diagrams for $\langle 0 \mid \mathcal{H}_{\alpha\mathrm{I}}\mathcal{O}_{01} \mid k; h\rangle$.

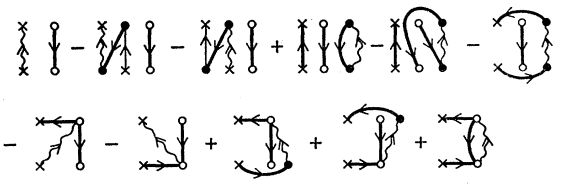

FIG. 8. A complete expression of diagrams for $\langle k'; h' \mid \mathcal{O}_{01}\mathcal{H}_{\alpha\mathrm{I}}\mathcal{O}_{01} \mid k; h\rangle$.

From this expression, it is obvious that diagrams containing m' pair-creation lines among the lower termini cancel each other on the right of (5.10). Nonvanishing contributions will appear only in the following situations. One possibility arises if at least one of m' pair-creation lines is replaced by a pair of overlap lines which connects the lower termini to the upper termini, provided $m''\geq 1$ in $\langle nm''A \mid$. Of course, one of the two overlap lines may be an interaction line as is the case in the first three diagrams in Fig. 5(a). Other possibilities appear if a pair-creation line is either replaced by an interaction line or linked to the interaction line by the interchange or cumulative overlapping mechanisms. Those three cases are illustrated by the three diagrams in the second row of Fig. 7. In conclusion, nonvanishing contributions appear only if one more pair of termini participates in connecting the two wave functions $\langle\cdots|$ and $|\cdots\rangle$.

Let us assume that a nonvanishing contribution to $\langle\cdots|\cdots\mathcal{H}_{\alpha\mathrm{I}}\mathcal{O}_{nm} \mid nm'A_p\rangle$ appears if at least $n+2m$ termini are involved in connecting the two wave functions. The assumption can be extended to the case where m is replaced by $m+1$, because Eq. (4.24) is generalized as follows:

$$\begin{aligned}&\langle\cdots|\cdots\mathcal{H}_{\alpha\mathrm{I}}\mathcal{O}_{nm+1} \mid nm'A_p\rangle \\ &\quad= \langle\cdots|\cdots\mathcal{H}_{\alpha\mathrm{I}}\mathcal{O}_{nm} \mid nm'A_p\rangle \\ &\quad- \langle\cdots|\cdots\mathcal{H}_{\alpha\mathrm{I}}\mathcal{O}_{nm} \mid nmA_{p_n}\rangle \\ &\qquad\times\langle 0A \mid 0\, m'-m\, A_{p_0}\rangle. \quad (5.11)\end{aligned}$$

This shows that nonvanishing contributions do not appear unless one more pair of lower termini contributes to the connection of the two wave functions. This proves the original assumption. The same arguments may be applied to the decomposition of $\langle nm''A_{p'} \mid \mathcal{O}_{nm'}\mathcal{H}_{\alpha\mathrm{I}}\cdots|\cdots\rangle$ as well as to matrices involving two-body interaction $\mathcal{H}_{\alpha\mathrm{II}}$. The conclusion may be summarized as follows.

Theorem 4. The normalization part of diagrams for $\langle nm'A_{p'} \mid \mathcal{O}_{nm'}\mathcal{H}_\alpha\mathcal{O}_{nm} \mid nmA_p\rangle$ consists of nothing but overlap lines which connect the lower termini to the upper termini. The nucleus of the linked interaction part is a self-energy diagram, a dynamical-interaction diagram, or a kinematical-interaction diagram. The latter type of diagrams appear only when one or two overlap or pair-creation lines are connected to a self-energy diagram by the interchange mechanism. Each solid dot involved in a linked interaction part may

connect a pair-creation line by the cumulative overlapping mechanism, yielding cumulant-correction diagrams. A diagram including pair-creation lines will vanish unless they are all connected to the linked interaction part.

The first statement of Theorem 4 implies that in each projected interaction-matrix element the normalization part contains the same number of lower and upper termini and the diagrams are exactly the same as those for the corresponding overlap-matrix element. Self-energy diagrams of one- and two-body interaction operators include, respectively, one and two heavy lines, and hence they can connect to only one and two more lines by the interchange mechanism. From Figs. 4 and 5(a), it will be found that the number of solid dots involved in self-energy and dynamical-interaction parts cannot exceed two if $\mathcal{H}_\alpha$ is a one-body operator and four if $\mathcal{H}_\alpha$ is a two-body operator. This imposes a limitation on the size of linked interaction parts. If an energy matrix of a one-body interaction is concerned, only three lines can be attached to the self-energy diagrams, one by the interchange and two by the cumulant-correction mechanism, the latter connecting one to the upper terminus and one to the lower terminus. In case of a two-body interaction, the number can be doubled. A dynamical-interaction diagram does not accommodate an extra line by the interchange mechanism since all possible permutations are already included in the diagrams in Fig. 5(a). In conclusion:

Corollary: Nonvanishing contributions from

$$\langle nm'A_{p'} \mid \mathcal{O}_{nm'}\mathcal{H}_\alpha\mathcal{O}_{nm} \mid nmA_p\rangle$$

will appear only if

$$\mid m-m' \mid \leq 2, \qquad \text{for } \mathcal{H}_\alpha=\mathcal{H}_{\alpha\mathrm{I}}, \tag{5.12a}$$

and

$$\mid m-m' \mid \leq 4, \qquad \text{for } \mathcal{H}_\alpha=\mathcal{H}_{\alpha\mathrm{II}}. \tag{5.12b}$$

Any of the diagrams generated following the above instructions will contain an interaction line representing a one- or two-body interacting integral

$$(l \mid \mathcal{H}^{(1)}(r) \mid h) \quad \text{or} \quad (l_1l_2 \mid \mathcal{H}^{(2)}(r_1, r_2) \mid h_1h_2).$$

Let us denote by

$$(l \mid \mathcal{H}^{(1)}(r) \mid h)\langle nm'A_{p'} \mid \mathcal{O}_{nm'}[l \mid h]\mathcal{O}_{nm} \mid nmA_p\rangle$$

or

$$(l_1l_2 \mid \mathcal{H}^{(2)}(r_1r_2) \mid h_1h_2) \times \langle nm'A_{p'} \mid \mathcal{O}_{nm'}[l_1l_2 \mid h_1h_2]\mathcal{O}_{nm} \mid nmA_p\rangle$$

the sum of all possible diagrams which include the particular integral

$$(l \mid \mathcal{H}^{(1)}(r) \mid h) \quad \text{or} \quad (l_1l_2 \mid \mathcal{H}^{(2)}(r_1r_2) \mid h_1h_2).$$

Then

$$\langle \cdots \mid \mathcal{O}_{nm'}[\cdots \mid \cdots]\mathcal{O}_{nm} \mid \cdots\rangle$$

represents not only the normalization parts of the diagrams, but also the portions of the linked interaction parts which consist of heavy lines and light lines. It is obvious that the projected interaction-matrix elements are expanded as

$$\begin{aligned}&\langle nm'A_{p'} \mid \mathcal{O}_{nm'}\mathcal{H}_\alpha\mathcal{O}_{nm} \mid nmA_p\rangle \\ &=\sum_h\sum_l (l \mid \mathcal{H}^{(1)}(r) \mid h)\langle nm'A_{p'} \mid \mathcal{O}_{nm'}[l \mid h]\mathcal{O}_{nm} \mid nmA_p\rangle \\ &\quad+\sum_{h_1}\sum_{h_2}\sum_{l_1}\sum_{l_2}(l_1l_2 \mid \mathcal{H}^{(1)}(r_1r_2) \mid h_1h_2) \\ &\quad\times\langle nm'A_{p'} \mid \mathcal{O}_{nm'}[l_1l_2 \mid h_1h_2]\mathcal{O}_{nm} \mid nmA_p\rangle.\end{aligned} \tag{5.13}$$

The expression is a generalization of (5.5) and (5.6) and may be obtained directly by the technique described in Ref. 4.

VI. CUMULANT REARRANGEMENT OF THE ENERGY MATRIX

Let us now calculate the energy matrix based on the orthonormal wave functions $\mathfrak{N} \mid nmp\rangle$ defined in the full space:

$$\begin{aligned}\mathfrak{N} \mid nmp\rangle &\equiv \mathfrak{N} \mid nmA_p\rangle\, \mathfrak{N} \mid -nmB_p\rangle \\ &\equiv \mathfrak{N} \mid k_1\cdots k_{m+n}; h_1\cdots h_m\rangle \\ &\quad\times \mathfrak{N} \mid h_1\cdots h_m; k_1\cdots k_{m+n}\rangle.\end{aligned} \tag{6.1}$$

Since excitations are assumed to be generated by permutations of spins, electrons taken out of G_α are always placed in G_β and vice versa, and electrons $k_1\cdots k_{m+n}$ and holes $h_1\cdots h_m$ in G_α are holes and electrons, respectively, in G_β. Hence, the same indices $k_1\cdots k_{m+n}$; $h_1\cdots h_m$ are repeated in $\mathfrak{N} \mid nmA_p\rangle$ and $\mathfrak{N} \mid -nmB_p\rangle$ in reverse order in (6.1).

A proper adaptation of the notation in (5.13) to the energy matrix yields that

$$\begin{aligned}&\langle nm'p' \mid \mathfrak{N}\mathcal{H}\mathfrak{N} \mid nmp\rangle \\ &\quad\equiv\langle\!|| \mathcal{H} ||\!\rangle \\ &\quad=\sum_j\sum_{j'}(j' \mid \mathcal{H}^{(1)}(r_1) \mid j)\langle\!||[j' \mid j]||\!\rangle \\ &\quad+\tfrac{1}{2}\sum_{j_1}\sum_{j_2}{}'\sum_{j_1'}\sum_{j_2'}{}'(j_1'j_2' \mid \mathcal{H}^{(2)}(r_1r_2) \mid j_1j_2) \\ &\qquad\times\langle\!||[j_1'j_2' \mid j_1j_2]||\!\rangle,\end{aligned} \tag{6.2}$$

where $||\rangle$ denotes $\mathfrak{N} \mid nmp\rangle$ and

$$\begin{aligned}\langle\!||[j_1'j_2' \mid j_1j_2]||\!\rangle &\equiv \langle nm'A_{p'} \mid \mathfrak{N}[j_1'j_2' \mid j_1j_2]\mathfrak{N} \mid nmA_p\rangle \\ &\quad\times\langle -nm'B_{p'} \mid \mathfrak{N}[j_1'j_2' \mid j_1j_2]\mathfrak{N} \mid -nmB_p\rangle,\end{aligned} \tag{6.3}$$

and

$$\begin{aligned}&\langle nm'A_{p'} \mid \mathfrak{N}[j_1'j_2' \mid j_1j_2]\mathfrak{N} \mid nmA_p\rangle \\ &\quad=\sum_{\bar{p}}\sum_{\bar{p}'}\langle nm'A_{p'} \mid \mathcal{O}_{nm'}{}^{-1/2} \mid nm'A_{\bar{p}'}\rangle \\ &\quad\times\langle nm'A_{\bar{p}'} \mid \mathcal{O}_{nm'}[j_1'j_2' \mid j_1j_2]\mathcal{O}_{nm} \mid nmA_{\bar{p}}\rangle \\ &\qquad\times\langle nmA_{\bar{p}} \mid \mathcal{O}_{nm}{}^{-1/2} \mid nmA_p\rangle.\end{aligned} \tag{6.4}$$

To transform the expression (6.2) into a more attractive form, let us decompose the one-body part of the Hamiltonian (5.2) as

$$\mathfrak{H}^{(1)}(r_1)=T(r_1)-\sum_j^{2N} V(r_1;R_j), \tag{6.5}$$

where $T(r_1)$ is the kinetic energy and $V(r_1;R_j)$ is the effective potential of the ion at R_j. In the Appendix, we shall show how the use of (6.5) in the first term on the right of (6.2) yields that

$$\begin{aligned} I_1=&\sum_i\sum_{j'}(j'\mid T(r_1)-V(r_1;R_j)\mid j)\langle\!\langle[\![j'\mid j]\!]\rangle\!\rangle \\ &-\sum_i\sum_{j''}'\sum_{j'}\sum_{j'''}'(j'j'''\mid V(r_1;R_{j''})\mid jj'')\\ &\times\langle\!\langle[\![j'j'''\mid jj'']\!]\rangle\!\rangle \\ &-2\sum_{(j\leftarrow j'')}\sum_{j'}\sum_{j'''}'(j'j'''\mid V(r_1;R_{j''})\mid jj)\\ &\times\langle\!\langle[\![j'j'''\mid jj]\!]\rangle\!\rangle, \end{aligned} \tag{6.6}$$

where $(j\leftarrow j'')$ denotes the ion pair in which two electrons are at atom j and none at atom j''. Since the set of indices j, j'', j', j''' involved in the second term on the right may be replaced by either j_1, j_2, j_1', j_2' or j_2, j_1, j_2', j_1', use of the resulting two expressions in (6.2) leads to

$$\begin{aligned} \langle\!\langle\,\mathfrak{H}\,\rangle\!\rangle=&\sum_j^{2N}\epsilon_j(nm'p';nmp)\\ &+\tfrac{1}{2}\sum_{j_1}\sum_{j_2}'\sum_{j_1'}\sum_{j_2'}'(j_1'j_2'\mid\mathfrak{H}(j_1j_2)\mid j_1j_2)\\ &\times\langle\!\langle[\![j_1'j_2'\mid j_1j_2]\!]\rangle\!\rangle\\ &+\sum_{(j_1\leftarrow j_2)}\sum_{j_1'}\sum_{j_2'}'(j_1'j_2'\mid\mathfrak{H}^0(j_1j_2)\mid j_1j_1)\\ &\times\langle\!\langle[\![j_1'j_2'\mid j_1j_1]\!]\rangle\!\rangle, \end{aligned} \tag{6.7}$$

where

$$\begin{aligned} \epsilon_j(nm'p';nmp)\equiv&\sum_{j'}(j'\mid T(r_1)-V(r_1;R_j)\mid j)\\ &\times\langle\!\langle[\![j'\mid j]\!]\rangle\!\rangle, \end{aligned} \tag{6.8}$$

$$\begin{aligned} \mathfrak{H}(j_1j_2)=&\mathfrak{H}^{(2)}(r_1r_2)-V(r_1;R_{j_2})-V(r_2;R_{j_1})\\ &+1/\mid R_{j_1}-R_{j_2}\mid, \end{aligned} \tag{6.9a}$$

and

$$\begin{aligned} \mathfrak{H}^0(j_1j_2)=&\mathfrak{H}^{(2)}(r_1r_2)-V(r_1;R_{j_2})-V(r_2;R_{j_2})\\ &+1/\mid R_{j_1}-R_{j_2}\mid. \end{aligned} \tag{6.9b}$$

The energy expression (6.7) is convenient for the system for one-electron atoms, each carrying a tightly bound electron and interacting weakly with each other. In fact, $\mathfrak{H}(j_1j_2)$ represents an interaction between two neutral atoms and ϵ_j the self-energy of an atom. If we use a solution φ of a single atom,

$$\{T(r_1)-V(r_1;R_j)\}\varphi(r_1-R_j)=\epsilon_0\varphi(r_1-R_j), \tag{6.10}$$

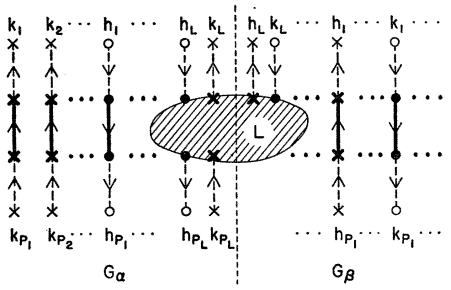

FIG. 9. A typical diagram for an energy matrix element.

as basis in the construction of the product function Φ defined by (2.2), the energy $\epsilon_j(nm'p';nmp)$ becomes exactly equal to the atomic energy ϵ_0 multiplied by $\delta_{mm'}\delta_{pp'}$.

Our object is to calculate the second term on the right of (6.7). Use of (6.3) and (6.4) reduces it to products of inverse overlap matrices $\langle\cdots\mid\mathcal{O}_{nm}^{-1/2}\mid\cdots\rangle$ and interaction matrices $\langle\cdots\mid\mathcal{O}_{nm'}[\cdots\mid\cdots]\mathcal{O}_{nm}\mid\cdots\rangle$.

The interaction matrices are calculated by the expansion technique developed in Sec. V, and the typical diagram is illustrated in Fig. 9, where the shaded portion indicates the linked interaction part $\mathfrak{L}_i$. We note that only a few termini are connected to the interaction part $\mathfrak{L}$; we shall call them *outgoing* (upper) or *incoming* (lower) *termini*. The interaction part appears only in G_α or G_β if the Hamiltonian is of the type (5.4a) but appears in both G_α and G_β if $\mathfrak{H}$ is of the type (5.4b). Under the summations $\sum_{j_1}\sum_{j_2}'\sum_{j_1'}\sum_{j_2'}'$ in (6.7), the energy integral $\langle nm'p'\mid\mathfrak{N}\cdots\mathfrak{N}\mid nmp\rangle$ is antisymmetric with respect to permutations of the indices k and h. Consequently, for each diagram there are $(m+n)!m!$ distinct ways to attach indices. Let us denote the permutations by the factor $(-1)^P$ and indices $k_{P_1}\cdots k_{P_{m+n}}h_{P_1}\cdots h_{P_m}$ in the diagram in Fig. 9.

A standard diagram for the overlap matrix $\langle\mid\mathcal{O}_{nm}^{-1/2}\mid\rangle$ given by (4.15) consists of broken lines connecting k_1 to k_1', $\cdots$, h_m to h_m'; other diagrams are all generated from the standard diagram by permutations of the termini of those broken lines. However, each diagram contributes identically to the energy expression (6.7) because of the antisymmetric properties of the interaction matrix. Hence, the inverse $\langle\mid\mathcal{O}_{nm}^{-1/2}\mid\rangle$ is given effectively by

$$\langle\mid\mathcal{O}_{nm}^{-1/2}\mid\rangle=\prod\prod(k_i'\mid\Gamma^{-1/2}\mid k_i)(h_j\mid\Delta^{1/2}\mid h_j'), \tag{6.11}$$

and only the standard diagrams shown in Fig. 9 are needed for these overlap matrices.

The summations $\sum_{\bar{p}}$ in (6.4) include

$$\binom{N}{n+m}\binom{N}{m}$$

terms generated from all possible distinct sets of indices

$k_1\cdots k_{m+n}$ and $h_1\cdots h_m$, and can be split into two parts, $\sum_{(\bar{L})}$ and $\sum_{(\bar{N})}$. The former $\sum_{(\bar{L})}$ is the sum over indices belonging to the linked interaction part, and the latter $\sum_{(\bar{N})}$ is the sum over indices involved in the normalization part. This will split the expression (6.4) schematically into a form like

$$(\sum_{(\bar{L})}^{G\alpha}{}' \sum_{(\bar{L}')}^{G\alpha}{}'\cdots)(\sum_{(\bar{N})}^{G\alpha}{}' \sum_{(\bar{N}')}^{G\alpha}{}'\cdots), \tag{6.12}$$

and consequently the energy matrix elements can also be split up as

$$\langle\!|| \mathcal{H} ||\!\rangle = \sum_{\substack{\text{all possible}\\ N\text{-}\bar{L}\text{ splits}}} \sum_i \langle L' || \mathfrak{L}_i || L\rangle_N \langle N' || N\rangle_L, \tag{6.13}$$

where the two factors on the right are formally given by

$$\langle L' || \mathfrak{L}_i || L\rangle_N = \sum_{(\bar{L})}^{G\alpha}{}' \sum_{(\bar{L}')}^{G\alpha}{}' \sum_{(\bar{L})}^{G\beta}{}' \sum_{(\bar{L}')}^{G\beta}{}' \langle L' \mid \mathfrak{O}^{-1/2} \mid \bar{L}'\rangle \times \langle \bar{L}' \mid \mathfrak{L}_i \mid \bar{L}\rangle\langle \bar{L} \mid \mathfrak{O}^{-1/2} \mid L\rangle \tag{6.14a}$$

and

$$\langle N' || N\rangle_L = \sum_{(\bar{N})}^{G\alpha}{}' \sum_{(\bar{N}')}^{G\alpha}{}' \sum_{(N)}^{G\beta}{}' \sum_{(N')}^{G\beta}{}' \langle N' \mid \mathfrak{O}^{-1/2} \mid \bar{N}'\rangle \times \langle \bar{N}' \mid \mathfrak{O} \mid \bar{N}\rangle\langle \bar{N} \mid \mathfrak{O}^{-1/2} \mid N\rangle. \tag{6.14b}$$

L and N represent indices involved in the linked interaction and normalization parts, respectively, that is,

$$L = k_{L'_1}\cdots h_{L'_1}\cdots;\ h_{L_1}\cdots k_{L_1}\cdots \tag{6.15a}$$

and

$$N = k_{N'_1}\cdots h_{N'_1}\cdots;\ h_{N_1}\cdots k_{N_1}\cdots. \tag{6.15b}$$

The indices in L and N (or L' and N') taken together are the same as the indices included in the wave function on the right (or left) of $\langle\!|| \mathcal{H} ||\!\rangle$.

Since each index appears either in $\sum'_{(\bar{L})}$ or $\sum'_{(\bar{N})}$, those two summations are not independent of each other, and $\langle L' || \mathfrak{L}_i || L\rangle_N$ and $\langle N' || N\rangle_L$ cannot be calculated separately. If the restrictions on the summations are disregarded, $\langle N' || N\rangle$ will become equivalent to the normalization condition of the basic functions $\mathfrak{N} \mid nmp\rangle$:

$$\langle N' || N\rangle \to \langle k_{N_1'}\cdots h_{N_1'}\cdots;\ h_{N_1}'\cdots k_{N_1}'\cdots \mid \mathfrak{N}^2 \mid k_{N_1'}\cdots h_{N_1'}\cdots;\ h_{N_1}\cdots k_{N_1}\cdots\rangle = [\delta(k_{N_1'}\cdots;\ k_{N_1}'\cdots)\delta(h_{N_1}\cdots;\ h_{N_1}'\cdots)]_{G\alpha}[\delta(h_{N_1'}\cdots;\ h_{N_1'}'\cdots)\delta(k_{N_1}\cdots;\ k_{N_1}'\cdots)]_{G\beta}, \tag{6.16}$$

where $[\cdots]_{G\alpha}$ includes δ functions among the indices involved in the G_α part of N and N'.

However, an extra diagram will be included erroneously whenever k or h, involved in the normalization part, coincides with one of the indices in the interaction part. Hence, the correct sum will be obtained if we construct such fictitious diagrams explicitly and subtract them from the unrestricted sum obtained above. To eliminate the normalization parts still remaining in those fictitious diagrams, the above process has to be repeated until all overlap lines are connected to the interaction parts. The linked diagrams generated in each of the processes are *cumulant-correction terms* similar to those introduced in Sec. V, but in place of pair-creation lines, overlap lines are involved in the present processes.

An example of the cumulant-correction diagrams is illustrated in Fig. 10, where a broken line on the right indicates that the two parts in the diagram are independent of each other and the summations associated with them are not restricted. The normalization part can then be replaced by (6.16), and the energy matrix elements may be written as

$$\langle\!|| \mathcal{H} ||\!\rangle = \sum_{\langle\cdots||} \sum_{||\cdots\rangle} \sum_i \langle k_{L'}'\cdots h_{L'}'\cdots;\ h_{L'}'\cdots k_{L'}'\cdots \,||\, \mathfrak{L}_i \,||\, k_{L'}\cdots h_{L'}\cdots;\ h_L\cdots k_L\cdots\rangle_{\text{cumul}}, \tag{6.17}$$

where $\sum_{||\cdots\rangle}$ includes not only the indices involved in the original sums $\sum_{(\bar{L})^{G\alpha}} \sum_{(\bar{L})^{G\beta}}$ but also others which have been connected to the interaction parts as the results of the cumulant corrections. This proves the linked cluster expansion of the Heitler–London method.

The calculation of the energy matrix elements may be summarized as follows.

(a) Construct linked interaction diagrams according to the instructions in Theorem 4 and the corollary. Diagrams are to be constructed in subspaces G_α and G_β simultaneously, and the open dots and crosses must be replaced by solid dots and heavy crosses. If $m=m'$, the type of diagrams in Fig. 8 will be generated in each space, while, for $m\neq m'$, diagrams like those in Fig. 7 will appear. Connect the outgoing and incoming termini with broken lines representing overlap integrals $(k_i' \mid \Gamma^{-1/2} \mid k_i)$ or $(h_j \mid \Delta^{1/2} \mid h_j')$ involved in $\langle\!| \mathfrak{O}^{-1/2} |\!\rangle$. The procedure is illustrated by the examples in Fig. 11.

(b) Generate cumulant-correction diagrams of the type shown in Fig. 10 and attach an extra factor -1 to each. Repeat the process and generate cumulant-correction diagrams in higher orders until all overlap lines are exhausted.

(c) Impose the orthogonality condition (6.16) on the indices not involved in the interaction part. Be-

cause of the structure of the orthogonality condition (6.16), the δ function for a particular set of indices, say, k_ik_i' (or h_jh_j'), can be eliminated only if the set of indices appears twice in the interaction diagram, once as an electron pair in G_α and once as a hole pair in G_β or vice versa. The resulting diagrams will contribute to energy matrix elements relating two distinct spin states.

(d) Numerical values of diagrams are obtained by inserting values of lines defined in Fig. 1. Solid dots and heavy crosses involved in the interaction parts represent the sum over all sites in the sublattices $[A]$ and $[B]$, respectively.

VII. PERTURBATION APPROACH

A. Effective Hamiltonian and the Perturbation Expansion

To formulate the many-body perturbation expansion, we need to introduce a set of creation and destruction operators. Let an operator A_k or A_h delete electron k or hole h which appears in $\mathfrak{N}\,|\,nmp\rangle$ when A_k or A_h operates on it, but erase $\mathfrak{N}\,|\,nmp\rangle$ if the index k or h is absent in $\mathfrak{N}\,|\,nmp\rangle$. That is,

$$A_l\mathfrak{N}\,|\cdots l\cdots\rangle=(-1)^{\nu(l)}\mathfrak{N}\,|\cdots\cdots\cdots\rangle, \quad (7.1a)$$

and

$$A_l\mathfrak{N}\,|\cdots\cdots\cdots\rangle=0, \quad (7.1b)$$

where l represents indices k and h, and $\mathrm{s}(l)$ is the number of indices, which precede l in $\mathfrak{N}\,|\cdots l\cdots\rangle$. The

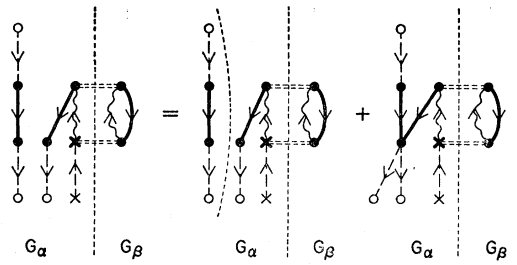

FIG. 10. Illustration of the cumulative overlapping mechanism.

Hermitian conjugate of A_l satisfies the expressions

$$A_l^\dagger\mathfrak{N}\,|\cdots\cdots\cdots\rangle=(-1)^{\nu(l)}\mathfrak{N}\,|\cdots l\cdots\rangle, \quad (7.2a)$$

and

$$A_l^\dagger\mathfrak{N}\,|\cdots l\cdots\rangle=0, \quad (7.2b)$$

because of the orthogonality of the bases. Operators B_k and B_h in G_β may be defined similarly. The operators A and B satisfy the anticommutation relations

$$[A_l^\dagger, A_{l'}]_+=[B_l^\dagger, B_{l'}]_+=\delta_{ll'}, \quad (7.3a)$$

$$[A_l^\dagger, A_{l'}^\dagger]_+=[A_l, A_{l'}]_+=[B_l^\dagger, B_{l'}^\dagger]_+=[B_l, B_{l'}]_+=0. \quad (7.3b)$$

The relations (7.1)–(7.3) illustrate that A, $A^\dagger$, B, and $B^\dagger$ are creation and destruction operators in G_α and G_β, respectively, of quasielectrons and holes defined by the orthonormal bases $\mathfrak{N}\,|\,nmp\rangle$. The energy calculation is then converted to the eigenvalue problem of the effective Hamiltonian:

$$\mathfrak{IC}_{\mathrm{eff}}=E_0+\sum_i \sum_{k'\cdots;\,h'\cdots}^{G_\alpha} \sum_{k\cdots;\,h\cdots}^{G_\alpha} \sum_{h'\cdots;\,k'\cdots}^{G_\beta} \sum_{h\cdots;\,k\cdots}^{G_\beta}$$
$$\times\langle k_{L'}'\cdots h_{L'}'\cdots;\, h_{L'}'\cdots k_{L'}'\cdots \,||\, \mathfrak{L}_i \,||\, k_{L'}\cdots h_{L'}\cdots;\, h_L\cdots k_L\cdots\rangle_{\mathrm{cumul}}$$
$$\times A_{k'L'}^\dagger\cdots B_{h'L'}^\dagger\cdots A_{h'L}^\dagger\cdots B_{k'L}^\dagger\cdots A_{kL'}\cdots B_{hL'}\cdots A_{hL}\cdots B_{kL}\cdots. \quad (7.4)$$

The values of $\langle||\,\mathfrak{L}_i\,||\rangle_{\mathrm{cumul}}$ may be evaluated by the instructions (a)–(d) in Sec. VI.[17]

The dominant contributions to $\mathfrak{IC}_{\mathrm{eff}}$ will undoubtedly come from the two-body Coulomb and exchange interactions. Figure 11 illustrates diagrams for the exchange interaction; diagrams generated from these by rotation through 180° should also be included. The type of diagrams in Fig. 11 is written as

$$\langle 0\,||\,\mathfrak{L}_i\,||\,kh;\,hk\rangle A_kB_hA_hB_k, \quad (7.5a)$$

while those obtained by the rotation represent the Hermitian conjugate of the above expression, that is,

$$\langle kh;\,hk\,||\,\mathfrak{L}_i\,||\,0\rangle A_k^\dagger B_h^\dagger A_h^\dagger B_k^\dagger. \quad (7.5b)$$

[17] To derive the value of an arbitrary matrix element, we should in principle, include an infinitely large number of overlap lines in the generation of cumulant-correction diagrams following instruction (b).

Simultaneous destruction of electron h in G_β and hole h in G_α denoted by A_hB_h is equivalent to a shift of electron h from G_β to G_α and may correspond to the raising operator S_h^+ in the Heisenberg theory. Similarly A_kB_k corresponds to the lowering operator S_k^-. The two terms in (7.5) are the *analog* of the anisotropic exchange Hamiltonian:

$$\sum_{k,h}\langle\cdots\rangle S_k^zS_h^z+\langle 0\,||\,\mathfrak{L}\,||\,kh;\,hk\rangle S_k^-S_h^+ +\langle kh;\,hk\,||\,\mathfrak{L}\,||\,0\rangle S_k^+S_h^- =-\sum_{k,h}J_{kh}[S_k^zS_h^z+\lambda(S_k^XS_h^X+S_k^YS_h^Y)]. \quad (7.6)$$

The first term is derived from the two-body Coulomb and exchange diagrams illustrated in Fig. 4(b) together with the cumulant-correction terms generated from them by attaching overlap lines carrying termini

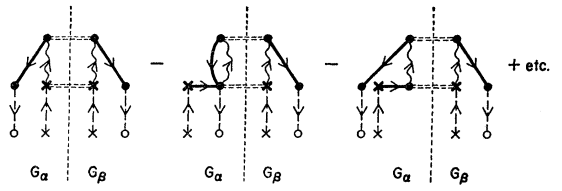

FIG. 11. Diagrams for the exchange interaction. The G_β parts of the diagrams will also take the other shapes which appear in the G_α parts of the second and third diagrams, leading to a total of nine diagrams.

$A_l^\dagger A_l(=N_l)$ or $B_l^\dagger B_l(=N_l)$. Those terms do not introduce interchanges of spins and correspond to the Ising Hamiltonian obtained when the spins are considered as classical vectors.

As we have pointed out in the introduction, the Hamiltonian (7.6) is a generalization of the Heisenberg spin Hamiltonian $H_{\text{spin}}(\lambda=1)$ obtained previously[4–6] and could include the Ising model. However, the differences are not limited to appearances only. Previously one could introduce only one kind of parameter, the exchange coupling constants J_{kh}, which are quantities characteristic of the quantum effect. Consequently, it is hard to justify that one can write the Hamiltonian as $H_{\text{spin}}(\lambda=0)$ when spins are considered as classical vectors. The present method describes the interactions $J_{kh}A_k^\dagger A_k B_h^\dagger B_h$, etc., as if they are static interactions between classical vectors, while the exchange couplings given by (7.5) are quantities characteristic of the quantum effect and given by matrix elements between two states generated by the corresponding interchanges of electrons.

Those differences are mainly due to the different projections of the motion of electrons into spin space. We note, however, that even for the simple Heitler–London case the present method already includes ionic structures through the orthogonalization procedure of the basic functions. Therefore, the exact result of (7.4) can be different from previously published results.[4–6]

The more complicated a diagram is, the less its value becomes, since each additional line introduces a factor of the order of an overlap integral.[18] This justifies the truncation of the effective Hamiltonian (7.4).

The ground-state energy can be evaluated by the perturbation expansion obtained by Goldstone.[10]

$$E=\sum_{r=0}^{\infty}\langle 0 \mid \mathfrak{H}_{\mathrm{I}}[(E_0-\mathfrak{H}_0)^{-1}\mathfrak{H}_{\mathrm{I}}]^r \mid 0\rangle_{\text{cumul}}, \quad (7.7)$$

where the precise definition of the cumulants $\langle\ \rangle_{\text{cumul}}$ is given in Ref. 12. It should be noted that the one-particle states defined by (6.8) and (6.10) are all degenerate and inappropriate to be used in the perturbation expansion for an unperturbed Hamiltonian $\mathfrak{H}_0$. Instead, the two-body term denoted by $\langle\cdots\rangle S_k^z S_h^z$ in (7.6) should be included in $\mathfrak{H}_0$.

The present method may be compared with the method in Ref. 12. The inclusion of the two-body static interactions in $\mathfrak{H}_0$ will greatly increase the convergence of the perturbation expansion but requires a generalization of Wick's theorem[19] to establish a prescription for the calculation of diagrams generated in the course of the perturbation expansion. The calculation in terms of fermion operators is, of course, simpler than the calculation involving spin operators.

B. Electron-Transfer Mechanism

Since excitations so far have been limited to permutations of spins, the δ function between a particular pair of indices appearing in (6.16) cannot be removed unless the pair appears in both G_α and G_β simultaneously as we have noted in the instruction (c) in Sec. VI. This restricts the summations in the effective Hamiltonian (7.4) and the type of diagrams.

If the restriction is disregarded and the two parts of each wave function, $\mathfrak{N} \mid nmA_p\rangle$ and $\mathfrak{N} \mid -nm'B_{p'}\rangle$ are constructed independently in G_α and G_β, each atom no longer carries an electron; some of them may carry one or two electrons and others none, and thus all possible ionic structures by charge transfers will be generated. These newly obtained functions are still orthonormal and the contributions appear as additional diagrams. The linked interaction parts in Fig. 10 illustrate typical examples of electron-transfer diagrams. They are written in the form

$$\sum_{k,h}[V_{kh}(A_kA_h+B_kB_h)+V_{hk}^*(A_h^\dagger A_k^\dagger+B_h^\dagger B_k^\dagger)]. \quad (7.8)$$

Intra-atomic interaction diagrams given by

$$\sum_l U_{ll}A_l^\dagger A_l B_l B_l^\dagger \quad (7.9)$$

will also appear whenever a pair of electrons occupies a single atom.

These interactions have been postulated in Hubbard's theory of narrow bands[8] and Anderson's theory of localized moments.[9] The present method provides an explicit prescription for the calculation of the interaction constants. We note that these terms are not expressible in terms of atomic spin operators nor can they be included in the Heisenberg theory of magnetism. In fact, the main object of the present paper is to develop a method of calculating localized electrons in which the electron-transfer mechanism and excitations of electrons in atoms are included so that the method

[18] More precisely, the order of magnitude of the linked interaction diagrams may be estimated easily. The cumulative overlapping mechanism will introduce additional pair-creation and/or overlap lines. Each pair-creation line yields at most a factor of the order of the nearest-neighbor overlap integral while each overlap line adds at most a factor of the order of the half-power of the next-nearest-neighbor overlap integral.

[19] Wick's theorem for interacting fermions is an obvious generalization of the theorem obtained in Ref. 12. See footnote 15 of Ref. 12.

can become an exact approach for the perturbation treatment of electrons in the insulating state. Although we have not discussed the method of including excitations of electrons, the extension may be carried out easily if we construct orthonormal basic functions by a technique similar to the one described in Sec. IV.

Physically, the operators A, $A^\dagger$, B, and $B^\dagger$ can be handled in exactly the same manner as the creation and destruction operators of the Wannier states. Because of the correlation built in the basic functions, the present method is free from the difficulties involved in the Wannier functions and can be used, for example, in an explicit calculation of the antiferromagnetic ground state. The successive orthogonalization introduced in Sec. IV ensures the maximum localization of electrons, while there is no exact proof of localization of the Wannier functions in the three-dimensional case.

C. Quasispin States

In the limit of large interatomic separations, both $\mathfrak{N} \mid nmp\rangle$ and the spin function Θ_{nmp} describe exactly the same spin state. As the distances become smaller, however, the magnitude of localized spins in $\mathfrak{N} \mid nmp\rangle$ may be screened by neighboring electrons with opposite spins due to the overlapping of charge densities of atomic orbitals. To illustrate this, let us calculate the spin density of the unperturbed ground state $\mid 0\rangle$. If the nearest-neighbor overlap integral is assumed to be appreciable but other overlap integrals are all considered negligible, overlap lines can be replaced by

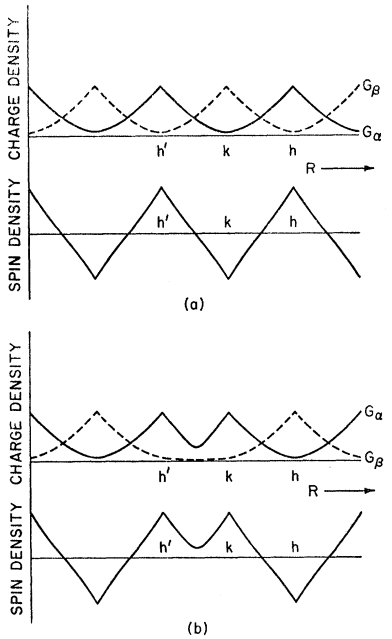

FIG. 12. Charge and spin densities of the basic functions $\mathfrak{N} \mid nmp\rangle$; (a) is for the unperturbed ground-state function $\mathfrak{N} \mid 0\rangle$ and (b) for $\mathfrak{N} \mid kh; hk\rangle$.

δ functions since orbitals are orthonormal within a sublattice. The density matrix for the spin-up part is then given by

$$\rho_{00}{}^{A}(1, 1') = \sum_h \mid h)(h \mid \Delta^{-1} \mid h)(h \mid + \sum_h \sum_{l \neq h} \mid l)(l \mid \Delta^{-1} \mid h)(h \mid = \sum_h \mid h)(h \mid, \tag{7.10}$$

and a similar expression for the spin-down part.

These charge distributions and the resulting net spin density are shown in Fig. 12(a). Since there is one electron per atom in the lattice, the sum of the two charge distributions within a Wigner–Seitz cell is unity while the spin density in the cell is given by the difference between those two distributions and is necessarily less than 1, illustrating the reduction of the net magnetic moment per atom in the quasispin state.

When the spins of electrons k and h are interchanged, the atom k and its neighbors h' will occupy the same spin states, and the cancellation of spin densities will not take place as is demonstrated in Fig. 12(b). More precisely, the charge density of the spin-up part is given by

$$\sum_{h' \neq h} \mid h')(h' \mid + \mid k)(k \mid - \tfrac{1}{2} \sum_h^{(k)} \{ \mid k)(k \mid h)(h \mid + \mid h)(h \mid k)(k \mid \}, \tag{7.11}$$

where $\sum_h{}^{(k)}$ includes all nearest neighbors of atom k. The last term comes from the second term of (7.10) and contributes only slightly to a partial cancellation of the spin densities.

This demonstrates that even in the simple Heitler-London scheme the present method deviates from the generalized Heisenberg theory. The basic functions $\mid nmp\rangle$ used here are different from and more realistic than the spin functions Θ_{nmp} used in the Heisenberg theory. Each atom in the unperturbed ground state carries a net magnetic moment which may be less than a Bohr magneton. An interchange of quasispins will not necessarily transfer the net magnetic moment, and the effective Hamiltonian $\mathfrak{IC}_{\text{eff}}$ is different from (7.6) even if only the two-body Coulomb and exchange interactions are retained and all other terms obtained by higher-order permutations are neglected in $\mathfrak{IC}_{\text{eff}}$. This is the reason why the truncated Hamiltonian $\mathfrak{IC}_{\text{eff}}$ could still be spin-isotropic even though it resembles the anisotropic spin Hamiltonian in appearance. Indeed, the magnetization may be calculated erroneously if one simply replaces the fermion operators in $\mathfrak{IC}_{\text{eff}}$ by atomic spin operators and solves the resulting spin Hamiltonian. In the Heisenberg theory, the fractional magnetization appears only as the result of spin correlation.

This shows that the present method cannot be applied for generation of a spin Hamiltonian in a rigorous manner.

APPENDIX

Since each atom involved in $|nmp\rangle$ carries a single electron, the matrix element $\langle nm'p'|\mathfrak{IC}^{(1)}(r)|nmp\rangle$ can be expanded similar to (6.6) but without the last term. In the course of the orthogonalization, however, many determinants, $|nm'A_{p'}\rangle$ and $|-nm''B_{p''}\rangle$ with m', $m''\leq m$, are added in $\mathfrak{N}|nmp\rangle$ and this creates a variety of ionic structures. Consequently (6.6) is no longer trivial. To prove (6.6), let us denote by $\bar{\jmath}$ the jth electron which is shifted from atom j to atom $\bar{\jmath}$. For singly occupied atoms, no electron transfers take place and hence $\bar{\jmath}=j$ and $\bar{\jmath}''=j''$ while $\bar{\jmath}''=\bar{\jmath}=j\neq j''$ illustrates that two electrons are at atom j and none at atom j''. We denote by $(j\leftarrow j'')$ the resulting ion pair.

The first term on the right of (6.2) is then written as

$$I=\sum_j\sum_{j'}(\bar{\jmath}'|T(r_1)-\sum_{j''}^{2N}V(r_1;R_{j''})|\bar{\jmath})\langle\|[\bar{\jmath}'|\bar{\jmath}]\|\rangle$$
$$=\sum_j\sum_{j'}(\bar{\jmath}'|T(r_1)-V(r_1;R_j)|\bar{\jmath})\langle\|[\bar{\jmath}'|\bar{\jmath}]\|\rangle$$
$$-\sum_j\sum_{j''}'\sum_{j'}\sum_{j'''}'(\bar{\jmath}'\bar{\jmath}'''|V(r_1;R_{j''})|\bar{\jmath}\bar{\jmath}'')$$
$$\times\langle\|[\bar{\jmath}'\bar{\jmath}'''|\bar{\jmath}\bar{\jmath}'']\|\rangle, \quad \text{(A1)}$$

where $\|\ \rangle$ represents $\mathfrak{N}|nmp\rangle$. Let us replace $V(r;R_{j''})$ for $\bar{\jmath}''\neq\bar{\jmath}$ and $V(r;R_j)$ in the above expression by $V(r;R_{\bar{\jmath}''})$ and $V(r;R_{\bar{\jmath}})$, respectively. Then (A1) becomes

$$I=\sum_j\sum_{j'}(\bar{\jmath}'|T(r_1)-V(r_1;R_{\bar{\jmath}})|\bar{\jmath})\langle\|[\bar{\jmath}'|\bar{\jmath}]\|\rangle-\sum_j\sum_{\substack{j''\\(\bar{\jmath}\neq\bar{\jmath}'')}}''\sum_{j'}\sum_{j'''}'(\bar{\jmath}'\bar{\jmath}'''|V(r_1;R_{\bar{\jmath}''})|\bar{\jmath}\bar{\jmath}'')\langle\|[\bar{\jmath}'\bar{\jmath}'''|\bar{\jmath}\bar{\jmath}'']\|\rangle$$
$$-2\sum_{(j\leftarrow j'')}\sum_{j'}\sum_{j'''}'(\bar{\jmath}'\bar{\jmath}'''|V(r_1;R_{j''})|jj)\langle\|[\bar{\jmath}'\bar{\jmath}'''|jj]\|\rangle+\Delta I, \quad \text{(A2)}$$

where ΔI results from the above replacement and is given by

$$\Delta I=\sum_j\sum_{j'}(\bar{\jmath}'|V(r_1;R_{\bar{\jmath}})-V(r_1;R_j)|\bar{\jmath})\langle\|[\bar{\jmath}'|\bar{\jmath}]\|\rangle$$
$$+\sum_j\sum_{\substack{j''\\(\bar{\jmath}\neq\bar{\jmath}'')}}''\sum_{j'}\sum_{j'''}'(\bar{\jmath}'\bar{\jmath}'''|V(r_1;R_{\bar{\jmath}''})-V(r_1;R_{j''})|\bar{\jmath}\bar{\jmath}'')\langle\|[\bar{\jmath}'\bar{\jmath}'''|\bar{\jmath}\bar{\jmath}'']\|\rangle$$
$$+\sum_{(j''\leftarrow j)}\sum_{j'}\sum_{j'''}'(\bar{\jmath}'\bar{\jmath}'''|V(r_1;R_j)-V(r_1;R_{j''})|j''j'')\langle\|[\bar{\jmath}'\bar{\jmath}'''|j''j'']\|\rangle$$
$$=\sum_j\sum_{j'}\sum_{\substack{j''\\(\bar{\jmath}\neq\bar{\jmath}'',j'')}}''(\bar{\jmath}'|V(r_1;R_{\bar{\jmath}''})-V(r_1;R_{j''})|\bar{\jmath})\langle\|[\bar{\jmath}'|\bar{\jmath}]\|\rangle. \quad \text{(A3)}$$

Note that the third term in the middle of (A3) appears when the term involving $(j''\leftarrow j)$ is reduced to the form of the third term in (A2). This term cancels the first term in (A3).

Contributions to ΔI will appear from terms like the second diagram in Fig. 11. The diagram shows that atomic orbital $k(=j'')$ is transformed to $h(\neq\bar{\jmath}'')$ in G_α but no electron transfer has taken place in G_β. As the result, there are two electrons at atom h but none at k and

$$\sum_j\sum_{j'}'(\bar{\jmath}'|V(r_1;R_h)-V(r_1;R_k)|\bar{\jmath})\langle\|[\bar{\jmath}'|\bar{\jmath}]\|\rangle \quad \text{(A4)}$$

is not zero. However, there is a diagram generated by the interchange of the G_α and G_β parts, in which two electrons are at atom k but none at atom h. Contributions of such diagrams to ΔI are obviously given by

$$\sum_j\sum_{j'}'(\bar{\jmath}'|V(r_1;R_k)-V(r_1;R_h)|\bar{\jmath})\langle\|[\bar{\jmath}'|\bar{\jmath}]\|\rangle. \quad \text{(A5)}$$

According to the properties of $\mathfrak{N}|nmp\rangle$ illustrated in (6.1), it is evident that for each diagram involving the ionic structure $(j\leftarrow j'')$, there exists a corresponding diagram of the same value with the reversed ionic structure $(j''\leftarrow j)$. Hence, the total contributions to ΔI vanish, and (A2) is equal to (6.6). This proves Eq. (6.6). A similar discussion may be applied to the calculation of the constant terms $1/|R_{j_1}-R_{j_2}|$ in (6.9).

If, as is discussed in Sec. VII B, the charge transfer is explicitly included in $\mathfrak{N}|nmp\rangle$, the above cancellation no longer holds. However, linear combinations of $\mathfrak{N}|nmp\rangle$ in which charge transfers $(j\leftarrow j'')$ as well as $(j''\leftarrow j)$ are equally included can be considered as the basic functions. Then ΔI vanishes and Eqs. (6.7)–(6.9) are still valid.